# Coxeter triangulations have good quality

Aruni Choudhary, Siargey Kachanovich, Mathijs Wintraecken

# Coxeter triangulations have good quality

Aruni Choudhary[1], Siargey Kachanovich[2], and Mathijs Wintraecken[2]

[1]Max Planck Institute for Informatics, Saarland Informatics Campus Saarbrücken, Germany
[2]Université Côte d'Azur, Inria, France

December 19, 2017

**Abstract**

Coxeter triangulations are triangulations of Euclidean space based on a simple simplex. By this we mean that given an individual simplex we can recover the entire triangulation of Euclidean space by inductively reflecting in the faces of the simplex. In this paper we establish that the quality of the simplices in all Coxeter triangulations is $O(1/\sqrt{d})$ of the quality of regular simplex. We further investigate the Delaunay property (and an extension thereof) for these triangulations. In particular, one family of Coxeter triangulations achieves the protection $O(1/d^2)$. We conjecture that both bounds are optimal for triangulations in Euclidean space.

# 1 Introduction

## 1.1 Objectives and motivation

Well shaped simplices are of importance for various fields of application such as finite element methods and manifold meshing [2, 9, 10, 20, 23, 30]. Poorly-shaped simplices may induce various problems in finite element method, such as large discretization errors or ill-conditioned stiffness matrices. A simplex is well shaped if its quality is good, which can be expressed in terms of various *quality measures*. Some examples of quality measures are: the ratio between minimal height and maximal edge length ratio called *thickness* [26, 34], the ratio between volume and a power of the maximal edge length called *fatness* [35], and the *inradius-circumradius ratio* [8]. Bounds on *dihedral angles* can also be included in the list of quality measures. We stress that there are many other quality measures in use and authors often find useful to introduce measures that are specific to whatever problem they study. Finding triangulations, even in Euclidean space, of which all simplices have good quality is a non-trivial exercise in arbitrary dimension.

In this paper we shall discuss Coxeter triangulations.

**Definition 1.1.** *A monohedral*[1] *triangulation is called* Coxeter triangulation *if all its $d$-simplices can be obtained by consecutive reflections through facets of the $d$-simplices in the triangulation.*

To our knowledge, these are the triangulations with the best quality in arbitrary dimension. In particular, all dihedral angles of simplices in Coxeter triangulations are $45°$, $60°$ or $90°$, with the exception of the so-called $\tilde{G}_2$ triangulation of the plane where we also can find an angle of $30°$. This is a clear sign of the exceptional quality of the simplices involved. Our goal is to exhibit the extraordinary properties of Coxeter triangulations and promote their use in the Computational Geometry community.

The self-similarity and symmetry are another of the attractive points of Coxeter triangulations. Upon the first introduction, an unprepared reader might expect that the vertex sets of such triangulations form lattices, however it is not necessarily true, as we show in Section 5.

We are also interested in the stronger requirement of *protection* [4], which is specific to Delaunay triangulations. For a point set to have a unique well defined Delaunay triangulation in the Euclidean space $\mathbb{R}^d$ one demands that there are no $d+2$ co-spherical points such that the interior of the sphere is empty in a vertex set. Protection requires not only that there is no other vertex on the (empty) circumsphere of $d+1$ vertices, but that any other vertex is at distance $\delta$ away from the circumsphere. It has been proven that protection guarantees good quality [4]. Some algorithms were introduced for the construction of a protected set, such as the perturbation-based algorithms in [5] and [6]. Both of these algorithms take a general $\varepsilon$-net in $\mathbb{R}^d$ as input and output a $\delta$-protected net with $\delta$ of the order just $\Omega(2^{-d^2}\varepsilon)$. An example of the $d$-dimensional Coxeter triangulation $\tilde{A}_d$ provides us another extremity. As we will see in the following, this highly-structured triangulation is Delaunay with protection $O(\frac{1}{d^2}\varepsilon)$. This protection value is the greatest in a general $d$-dimensional Delaunay triangulation we know.

[1]A triangulation of $\mathbb{R}^d$ is called *monohedral* if all its $d$-simplices are congruent.

## 1.2 Related work

The notion of Coxeter triangulations was introduced to the computational geometry community by Dobkin, Wilks, Levy and Thurston in [16], where they tackled the problem of contour-tracing in $\mathbb{R}^d$. The choice of Coxeter triangulations was motivated by the following requirements:

- It should be easy to find the simplex that shares a facet with a given simplex.
- It should be possible to label the vertices of all the simplices at the same time with indices $0, \ldots, d$, in such a way that each of the $d+1$ vertices of a $d$-simplex has a different label.
- The triangulations should be homogeneous, meaning that all simplices are congruent.
- All simplices should be isotropic, meaning that they should be roughly the same in all directions.

Thanks to the definition, this is exactly what Coxeter triangulations do. After comparing the inradius-circumradius ratio of the simplices in the triangulations they chose the $\tilde{A}_d$ Coxeter triangulation as the underlying triangulation for their contour-tracing algorithm.

Adams, Baek and Davis [1] chose the vertex set of $\tilde{A}_d$ Coxeter triangulation, also known as the *permutahedral lattice*, to accelerate the high-dimensional Gaussian filtering algorithm. This choice was again motivated by the fact that the triangulation has congruent and isotropic simplices.

The $\tilde{A}_d$ Coxeter triangulation was also used to approximate the Rips filtration of $n$ points in $\mathbb{R}^d$ in a recent work by Choudhary, Kerber and Raghvendra [11]. The authors arrived at an approximation scheme that achieved a significant reduction in size of the complex. The improvement came primarily from the fact that the permutahedral lattice is very well protected.

Coxeter triangulations also played an important role in [3, 19].

The Coxeter triangulations we study are intricately linked with root systems and root lattices. Delaunay triangulations of the root lattices have been studied by Conway and Sloane [12] and Moody and Patera [25]. These triangulations are different from the ones we study: the vertex sets we use are not necessarily lattices.

The three-dimensional Coxeter triangulation $\tilde{A}_3$ has attracted attention in the 3D mesh generation community for the high-quality of its simplices. The vertex set of this triangulation is also known as the *body-centred cubic lattice*, or bcc lattice, and its tetrahedron is sometimes referred as *Sommerville's type II tetrahedron* (after [29]) or simply bcc-tetrahedron. This tetrahedron has been shown in [27] to be the best-conditioned space-filling tetrahedron out of all space-filling tetrahedra used in the 3D mesh community by a number of conditioning measures. This work led to the use of the bcc lattice in the isosurface stuffing algorithm [24].

Other examples of the use of the bcc lattice include the optimal sampling in image processing [31] and improving on the marching tetrahedra algorithm for isosurface extraction [33]. In both papers the main reason behind the choice of the bcc lattice was its sparse covering. This makes the sampling algorithm achieve the same accuracy as the usual cubic lattice with about 29.3% fewer samples.

Lastly, an observation that a bcc tetrahedron can be divided into eight half-sized bcc tetrahedra was used to make a variation of the octree algorithm [17].

## 1.3 Contribution

In this paper we give explicit expressions of a number of quality measures of Coxeter triangulations for all dimensions, presented in Section 5. This is an extension of the work by Dobkin et al. [16] who presented a table of the values of the inradius-circumradius ratio for the Coxeter triangulations up to dimension 8. We also provide explicit measures of the corresponding simplices in Appendix B, allowing the reader to compute quality measures other than the ones listed.

In Section 3, we state the theorem of optimality of the regular $d$-simplex for each of the chosen quality measures. This theorem gives us right to work with normalized versions of these quality measures.

In Section 4, we established a criterion to identify if any given monohedral triangulation is Delaunay.

We also give a presentation of the theory of root systems in Appendix A. This presentation mostly follows the lecture notes of Jaap Top (in Dutch) [32] and a classical book by Humphreys [18] for the part on affine Weyl groups.

## 1.4 Future work

The simplex qualities, defined in Definition 3.1, of the four families of Coxeter triangulations behave as $O(1/\sqrt{d})$ in terms of dimension. We conjecture that this quality is optimal for a general space-filling triangulation in $\mathbb{R}^d$. In addition, the $d$-dimensional Coxeter triangulation $\tilde{A}_d$ has the relative Delaunay protection $O(1/d^2)$. We further conjecture that it is optimal for a general space-filling triangulation in $\mathbb{R}^d$. These conjectures are motivated by the extraordinary lower and upper bounds on the dihedral angles of simplices in Coxeter triangulations, they

are precisely 45°, 60° or 90° for the four families. Moreover the circumcentre of the simplices of $\tilde{A}_d$ lie very far inside the simplex.

# 2 Brief introduction to Coxeter triangulations

In this section we will give all the information about Coxeter triangulations, necessary for the understanding of the later sections. For the extended introduction we refer the reader to Appendix A, but also to the pioneering paper on reflection groups by Coxeter [14] and the classical book on Lie groups and algebras by Bourbaki [7]. Another classical reference book is "Sphere packings, Lattices, and Groups" by Conway and Sloane [12], upon which we draw for our geometric analysis of triangulations in Appendix B.

As we see in Appendices A.4 and A.5, the definition of Coxeter triangulations restricts the possible dihedral angles of the corresponding simplices. Indeed, the only possible dihedral angles are $\frac{\pi}{2}$, $\frac{\pi}{3}$, $\frac{\pi}{4}$ and $\frac{\pi}{6}$. This information can be represented in a graph.

**Definition 2.1.** *Let $\mathcal{T}$ be a Coxeter triangulation in $\mathbb{R}^d$ and $\sigma \in \mathcal{T}$ be its $d$-simplex. The* Coxeter diagram *of $\sigma$ consists of a graph with the following data. For each facet $\tau$ of $\sigma$ we insert one vertex. For every pair $(\tau, \tau')$ of facets in $\sigma$ we define a number $m(\tau, \tau') \in \{2, 3, 4, 6\}$, such that the dihedral angle $\varphi$ between $\tau$ and $\tau'$ satisfies $\varphi = \frac{\pi}{m(\tau,\tau')}$. We then insert an edge between $\tau$ and $\tau'$ and write the number $m(\tau, \tau')$ next to it.*
*We further follow the convention not to draw an edge labelled 2 and not denote the label 3 next to an edge.*

*The Coxeter diagram of $\mathcal{T}$ is the Coxeter diagram of any of its simplices.*

There are exactly four families of Coxeter diagrams and five exceptional diagrams.

**Theorem 2.2.** *The complete list of Coxeter diagrams is given in Figure 1.*

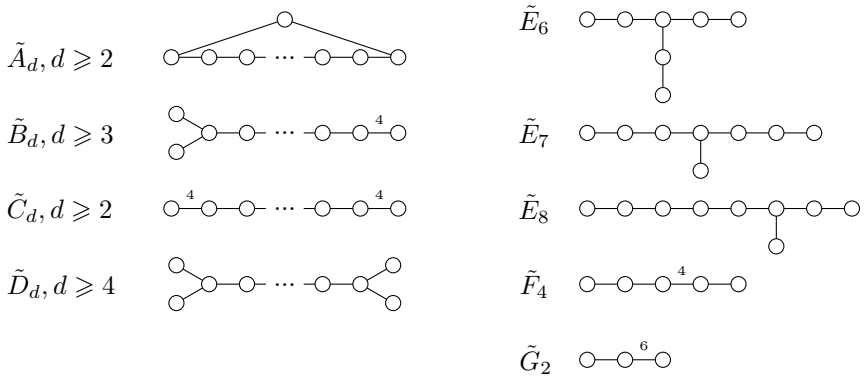


Figure 1: List of all Coxeter diagrams.

The vertices of simplices that correspond to these Coxeter diagrams up to similarity transformations are given in Table 1.

All three two-dimensional Coxeter triangulations are presented in Figure 2. Figure 3 illustrates the simplices of the three-dimensional Coxeter triangulations with vertices placed in vertices, centres of edges, centres of faces and at the centre of a cube.

# 3 Quality definitions

The quality measures we are interested in, we call *aspect ratio*, *fatness*, *thickness* and *radius ratio*. Their formal definitions are as follows:

**Definition 3.1.** *Let $h(\sigma)$ denote the minimal height, $r(\sigma)$ the inradius, $R(\sigma)$ the circumradius, $vol(\sigma)$ the volume and $L(\sigma)$ the maximal edge length of a given $d$-simplex $\sigma$.*

- *The* aspect ratio *of $\sigma$ is the ratio of its minimal height to the diameter of its circumscribed ball: $\alpha(\sigma) = \frac{h(\sigma)}{2R(\sigma)}$.*
- *The* fatness *of $\sigma$ is the ratio of its volume to its maximal edge length taken to the power $d$: $\Theta(\sigma) = \frac{vol(\sigma)}{L(\sigma)^d}$.*
- *The* thickness *of $\sigma$ is the ratio of its minimal height to its maximal edge length: $\theta(\sigma) = \frac{h(\sigma)}{L(\sigma)}$.*

| | |
|---|---|
| $\tilde{A}_d$, given in $\mathbb{R}^{d+1}$, $d \geq 2$ | $u_0 = \left(0^{\{d+1\}}\right)$<br>$u_k = \left((-\frac{d+1-k}{d+1})^{\{k\}}, (\frac{k}{d+1})^{\{d+1-k\}}\right), \quad \forall k \in \{1, \ldots, d\}$ |
| $\tilde{B}_d$, given in $\mathbb{R}^d$, $d \geq 3$ | $u_0 = \left(0^{\{d\}}\right)$<br>$u_1 = \left(1, 0^{\{d-1\}}\right)$<br>$u_k = \left(\frac{1}{2}^{\{k\}}, 0^{\{d-k\}}\right), \forall k \in \{2, \ldots, d\}$ |
| $\tilde{C}_d$, given in $\mathbb{R}^d$, $d \geq 2$ | $u_k = \left(\frac{1}{2}^{\{k\}}, 0^{\{d-k\}}\right), \forall k \in \{0, \ldots, d\}$ |
| $\tilde{D}_d$, given in $\mathbb{R}^d$, $d \geq 4$ | $u_0 = \left(0^{\{d\}}\right)$<br>$u_1 = \left(1, 0^{\{d-1\}}\right)$<br>$u_k = \left(\frac{1}{2}^{\{k\}}, 0^{\{d-k\}}\right), \forall k \in \{2, \ldots, d-2\}$<br>$u_{d-1} = \left(\frac{1}{2}^{\{d-1\}}, -\frac{1}{2}\right)$<br>$u_d = \left(\frac{1}{2}^{\{d\}}\right)$ |
| $\tilde{E}_6$, given in $\mathbb{R}^8$ | $u_0 = \left(0^{\{8\}}\right)$<br>$u_1 = \left(0^{\{5\}}, -\frac{2}{3}^{\{2\}}, \frac{2}{3}\right)$<br>$u_2 = \left(\frac{1}{4}^{\{5\}}, -\frac{1}{4}^{\{2\}}, \frac{1}{4}\right)$<br>$u_3 = \left(-\frac{1}{4}, \frac{1}{4}^{\{4\}}, -\frac{5}{12}^{\{2\}}, \frac{5}{12}\right)$<br>$u_4 = \left(0^{\{2\}}, \frac{1}{3}^{\{3\}}, -\frac{1}{3}^{\{2\}}, \frac{1}{3}\right)$<br>$u_5 = \left(0^{\{3\}}, \frac{1}{2}^{\{2\}}, -\frac{1}{3}^{\{2\}}, \frac{1}{3}\right)$<br>$u_6 = \left(0^{\{4\}}, 1, -\frac{1}{3}^{\{2\}}, \frac{1}{3}\right)$ |
| $\tilde{E}_7$, given in $\mathbb{R}^8$ | $u_0 = \left(0^{\{8\}}\right)$<br>$u_1 = \left(0^{\{6\}}, \frac{1}{2}, -\frac{1}{2}\right)$<br>$u_2 = \left(-\frac{1}{4}^{\{6\}}, \frac{1}{2}, -\frac{1}{2}\right)$<br>$u_3 = \left(\frac{1}{6}, -\frac{1}{6}^{\{5\}}, \frac{1}{2}, -\frac{1}{2}\right)$<br>$u_4 = \left(0^{\{2\}}, -\frac{1}{4}^{\{4\}}, \frac{1}{2}, -\frac{1}{2}\right)$<br>$u_5 = \left(0^{\{3\}}, -\frac{1}{3}^{\{3\}}, \frac{1}{2}, -\frac{1}{2}\right)$<br>$u_6 = \left(0^{\{4\}}, -\frac{1}{2}^{\{2\}}, \frac{1}{2}, -\frac{1}{2}\right)$<br>$u_7 = \left(0^{\{5\}}, -1, \frac{1}{2}, -\frac{1}{2}\right)$ |
| $\tilde{E}_8$, given in $\mathbb{R}^8$ | $\vec{u}_0 = \left(0^{\{8\}}\right)$<br>$\vec{u}_1 = \left(0^{\{7\}}, 1\right)$<br>$\vec{u}_2 = \left(\frac{1}{6}^{\{7\}}, \frac{5}{6}\right)$<br>$\vec{u}_3 = \left(-\frac{1}{8}, \frac{1}{8}^{\{6\}}, \frac{7}{8}\right)$<br>$\vec{u}_4 = \left(0^{\{2\}}, \frac{1}{6}^{\{5\}}, \frac{5}{6}\right)$<br>$\vec{u}_5 = \left(0^{\{3\}}, \frac{1}{5}^{\{4\}}, \frac{4}{5}\right)$<br>$\vec{u}_6 = \left(0^{\{4\}}, \frac{1}{4}^{\{3\}}, \frac{3}{4}\right)$<br>$\vec{u}_7 = \left(0^{\{5\}}, \frac{1}{3}^{\{2\}}, \frac{2}{3}\right)$<br>$\vec{u}_8 = \left(0^{\{6\}}, \frac{1}{2}^{\{2\}}\right)$ |
| $\tilde{F}_4$, given in $\mathbb{R}^4$ | $u_0 = (0, 0, 0, 0)$<br>$u_1 = \left(\frac{1}{2}, \frac{1}{2}, 0, 0\right)$<br>$u_2 = \left(\frac{2}{3}, \frac{1}{3}, \frac{1}{3}, 0\right)$<br>$u_3 = \left(\frac{3}{4}, \frac{1}{4}, \frac{1}{4}, \frac{1}{4}\right)$<br>$u_4 = (1, 0, 0, 0)$ |
| $\tilde{G}_2$, given in $\mathbb{R}^2$ | $u_0 = (0, 0)$<br>$u_1 = (1, 0)$<br>$u_2 = \left(1, \sqrt{3}\right)$ |

Table 1: Vertices of a simplex per Coxeter diagram type. Although a partial list has been provided by Conway and Sloane [12] we are not aware of any complete explicit overview. We believe that such a list will be of essential for many practitioners. The powers in point coordinates correspond to duplications of the same coordinate, for example $(\frac{1}{2}^{\{3\}}, -\frac{1}{2})$ is the same as $(\frac{1}{2}, \frac{1}{2}, \frac{1}{2}, -\frac{1}{2})$.

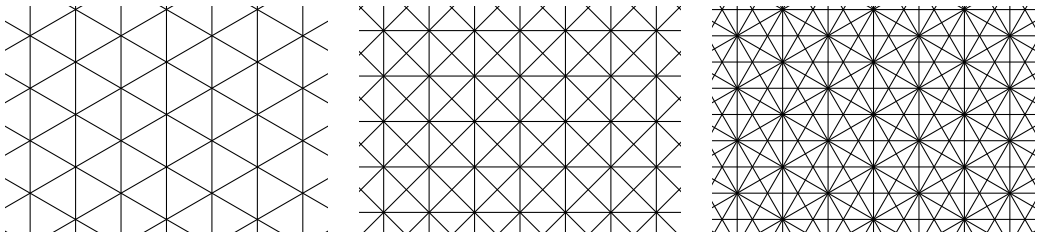

$\tilde{A}_2$ $\tilde{C}_2$ $\tilde{G}_2$

Figure 2: Coxeter triangulations in $\mathbb{R}^2$.

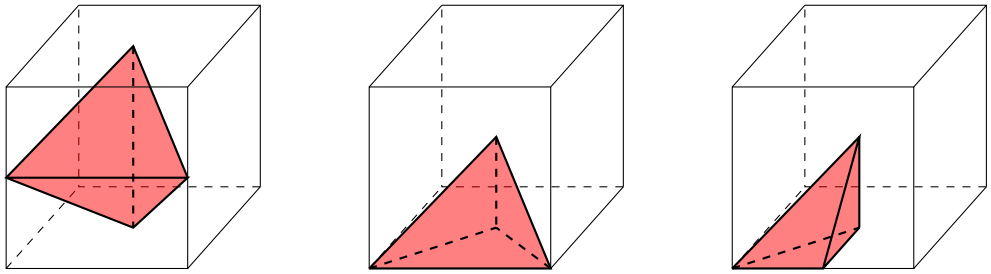

$\tilde{A}_3$ $\tilde{B}_3$ $\tilde{C}_3$

Figure 3: Simplices of Coxeter triangulations in $\mathbb{R}^3$ represented as a portion of a cube.

- *The* radius ratio *of $\sigma$ is the ratio of its inradius to its circumradius:* $\rho(\sigma) = \frac{r(\sigma)}{R(\sigma)}$.

To be able to compare the presented quality measures between themselves, we will normalize them by their respective maximum value. As we show in Appendix C, all of these quality measures are maximized by regular simplices.

**Theorem 3.2.** *Out of all $d$-dimensional simplices, the regular $d$-simplex has the highest aspect ratio, fatness, thickness and radius ratio.*

For a quality measure $\kappa$ we will define the normalized quality measure $\hat{\kappa}$, such that for each $d$-simplex $\sigma$, $\hat{\kappa}(\sigma) = \frac{\kappa(\sigma)}{\kappa(\Delta)}$, where $\Delta$ is the regular $d$-simplex. Theorem 3.2 ensure that the quality measures $\hat{\rho}$, $\hat{\alpha}$, $\hat{\theta}$ and $\hat{\Theta}$ take their values in $[0, 1]$ surjectively.

# 4 Delaunay criterion for Coxeter triangulations

Many of the provably good mesh generation algorithms are based on Delaunay triangulations [10]. This motivated us to investigate if Coxeter triangulations have the Delaunay property. In order to establish that, we need several criteria for triangulations to be (or not to be) Delaunay.

**Definition 4.1.** *A simplex is called* self-centred *if it contains its circumcentre inside or on the boundary.*

We have that:

**Lemma 4.2** ([28, Theorem 5])**.** *If a triangulation of $\mathbb{R}^d$ consists of only self-centred simplices, then it is a Delaunay triangulation.*

By definition, all Coxeter triangulations are monohedral. This means that it is sufficient to check if one simplex in the triangulation is self-centred to conclude that the triangulation is Delaunay.

**Corollary 4.3.** *If a simplex in a Coxeter triangulation is self-centred, then this triangulation is Delaunay.*

We now want to consider the converse:

**Lemma 4.4.** *Let $R$ be the maximum circumradius in a Delaunay triangulation $\mathcal{D}$ of $\mathbb{R}^d$. Then any simplex in $\mathcal{D}$ with circumradius $R$ is self-centred.*

The proof of Lemma 4.4 can be found in Appendix D.

All Coxeter triangulations are monohedral, therefore all simplices have the same circumradius. So trivially all the simplices have the maximum circumradius in the triangulation. This observation along with Lemma 4.4 leads us to conclude that if a simplex in a Coxeter triangulation is not self-centred, then the triangulation is not Delaunay. By combining this with Corollary 4.3 yields:

**Theorem 4.5.** *A Coxeter triangulation is Delaunay if and only if its simplices are self-centred.*

Because some of the triangulations that interest us here are Delaunay, we will also look at their *protection* value.

**Definition 4.6.** *The* protection *of a $d$-simplex $\sigma$ in a Delaunay triangulation on a point set $P$ is the minimal distance of points in $P \setminus \sigma$ to the circumscribed ball of $\sigma$:*

$$\delta(\sigma) = \inf_{p \in P \setminus \sigma} d(p, B(\sigma)), \text{ where } B(\sigma) \text{ is the circumscribed ball of } \sigma.$$

*The* protection *$\delta$ of a Delaunay triangulation $\mathcal{T}$ is the infimum over the $d$-simplices of the triangulation: $\delta = \inf_{\sigma \in \mathcal{T}} \delta(\sigma)$.*

We define the *relative protection* $\hat{\delta}(\sigma)$ of a given $d$-simplex $\sigma$ to be the ratio of the protection to its circumscribed radius: $\hat{\delta}(\sigma) = \frac{\delta(\sigma)}{R(\sigma)}$.

The *relative protection* $\hat{\delta}$ of a Delaunay triangulation $\mathcal{T}$ is the infimum over the $d$-simplices of the triangulation: $\hat{\delta} = \inf_{\sigma \in \mathcal{T}} \hat{\delta}(\sigma)$.

In the spirit of Theorem 4.5, we can easily spot if a Coxeter triangulation is not protected with the help of the following lemma:

**Lemma 4.7.** *A Delaunay triangulation where the simplex with maximal circumradius contains the circumcentre on its boundary is not protected.*

We prove this lemma in Appendix D.

Again, by using the fact that Coxeter triangulations are monohedral, we derive from the previous lemma the following theorem:

**Theorem 4.8.** *If a simplex of a Coxeter triangulation contains the circumcentre on its boundary, then the triangulation is non-protected Delaunay.*

Finally, one can slightly modify Lemma 8 and Theorem 5 in [28] by replacing all non-strict inequalities to strict inequalities to get a criterion for a non-zero protection:

**Theorem 4.9.** *If a simplex of a Coxeter triangulation contains the circumcentre strictly inside, then the triangulation is Delaunay with a non-zero protection.*

# 5 Main result

In this section we present a summarized table with explicit expressions of quality measures of Coxeter triangulations. In addition to that we also identify which Coxeter triangulations are Delaunay and give their protection values. Finally, we identify which Coxeter triangulations have vertex sets with lattice structure.

**Theorem 5.1.** *The normalized fatness, aspect ratio, thickness and radius ratio of simplices in Coxeter triangulations, as well as Delaunay property are:*

| | *Fatness* $\hat{\Theta}^{1/d}$ | *Aspect Ratio* $\hat{\alpha}$ | *Thickness* $\hat{\theta}$ | *Radius Ratio* $\hat{\rho}$ | *Delaunay?* |
|---|---|---|---|---|---|
| $\tilde{A}_d$, *d odd* | $\frac{2^{3/2}}{\left(\sqrt{d+1}\right)^{1+2/d}}$ | $\sqrt{\frac{6d}{(d+1)(d+2)}}$ | $\frac{2\sqrt{d}}{d+1}$ | $\sqrt{\frac{6d}{(d+1)(d+2)}}$ | ✓ |
| $\tilde{A}_d$, *d even* | $\frac{2^{3/2}(\sqrt{d+1})^{1-2/d}}{\sqrt{d(d+2)}}$ | | $\frac{2}{\sqrt{d+2}}$ | | |
| $\tilde{B}_d$ | $\frac{2^{1/2+1/d}}{\sqrt{d}\left(\sqrt{d+1}\right)^{1/d}}$ | $\frac{d\sqrt{2}}{(d+1)\sqrt{d+2}}$ | $\frac{1}{\sqrt{d+1}}$ | $\frac{2d}{\sqrt{d+2}(1+(d-1)\sqrt{2})}$ | ✗ |
| $\tilde{C}_d$ | $\frac{\sqrt{2}}{\sqrt{d}\left(\sqrt{d+1}\right)^{1/d}}$ | $\frac{\sqrt{2d}}{d+1}$ | $\frac{1}{\sqrt{d+1}}$ | $\frac{2\sqrt{d}}{2+(d-1)\sqrt{2}}$ | ✓ |
| $\tilde{D}_d$ | $\frac{2^{1/2+2/d}}{\sqrt{d}\left(\sqrt{d+1}\right)^{1/d}}$ | $\frac{d\sqrt{2}}{(d+1)\sqrt{d+4}}$ | $\frac{1}{\sqrt{d+1}}$ | $\frac{d\sqrt{2}}{(d-1)\sqrt{d+4}}$ | ✗ |
| $\tilde{E}_6$ | $\sqrt[12]{\frac{64}{137781}}$ | $\frac{2}{7}$ | $\frac{1}{\sqrt{14}}$ | $\frac{1}{2}$ | ✗ |
| $\tilde{E}_7$ | $\sqrt[14]{\frac{1}{177147}}$ | $\frac{7\sqrt{13}}{104}$ | $\frac{\sqrt{21}}{24}$ | $\frac{14\sqrt{13}}{117}$ | ✗ |
| $\tilde{E}_8$ | $\sqrt[8]{\frac{1}{3240}}$ | $\frac{8\sqrt{19}}{171}$ | $\frac{2\sqrt{19}}{57}$ | $\frac{8\sqrt{19}}{95}$ | ✗ |
| $\tilde{F}_4$ | $\sqrt[8]{\frac{1}{405}}$ | $\frac{4\sqrt{2}}{15}$ | $\frac{2\sqrt{5}}{15}$ | $\frac{4\sqrt{2}}{3(2+\sqrt{2})}$ | ✓ |
| $\tilde{G}_2$ | $\frac{\sqrt{2}}{2}$ | $\frac{1}{\sqrt{3}}$ | $\frac{1}{2}$ | $\frac{2}{1+\sqrt{3}}$ | ✓ |

*Out of them, only $\tilde{A}$ family triangulations have a non-zero relative protection value equal to:*

$$\hat{\delta} = \frac{\sqrt{d^2+2d+24} - \sqrt{d^2+2d}}{\sqrt{d^2+2d}} \sim \frac{12}{d^2}$$

*Only $\tilde{A}$ family, $\tilde{C}$ family and $\tilde{D}_4$ triangulations have vertex sets with lattice structure.*

The proof of this theorem and the table without normalization can be found in Appendix B.

The corresponding quality measures for the regular $d$-simplex $\Delta$ (which does not correspond to a triangulation in general) are:

| | Fatness $\Theta$ | Aspect Ratio $\alpha$ | Thickness $\theta$ | Radius Ratio $\rho$ |
|---|---|---|---|---|
| $\Delta$ | $\frac{1}{d!}\sqrt{\frac{d+1}{2^d}}$ | $\frac{d+1}{2d}$ | $\sqrt{\frac{d+1}{2d}}$ | $\frac{1}{d}$ |

All simplex quality measures in the table above are normalized with respect to the regular simplex. Note that the fatness values in the table are given powered $1/d$. It is due to the fact that fatness is a volume-based simplex quality. Also note that all normalized simplex qualities for the families $\tilde{A}_d$, $\tilde{B}_d$, $\tilde{C}_d$ and $\tilde{D}_d$ behave as $O\left(\frac{1}{\sqrt{d}}\right)$.

The numerical values of these quality measures are given in Tables 3, 4, 5 and 6 in Appendix E, and plotted in Figure 4 below. A quick glance suffices to see that $\tilde{A}_d$ achieves the greatest aspect ratio, fatness, thickness and radius ratio among the Coxeter triangulations in each dimension $d$.

# 6 Protection value of an $\tilde{A}_d$ triangulation

In this section we will prove the bound on protection stated in Theorem 5.1.

**Lemma 6.1.** *$\tilde{A}_d$ Coxeter triangulation has a relative protection equal to*

$$\hat{\delta} = \frac{\sqrt{d^2+2d+24} - \sqrt{d^2+2d}}{\sqrt{d^2+2d}} \sim \frac{12}{d^2}.$$

*Proof.* Let $V$ be the vertex set of the triangulation containing the simplex in the $\tilde{A}_d$ row of Table 1. By Proposition B.2 in Appendix B, $V$ coincides with the coweight lattice, which corresponds to an $A_d$ root system $R$.

Take the following basis vectors of the coweight lattice $V$:

$$\vec{u}_k = \frac{1}{d+1}\left((k-(d+1))^{\{k\}}, k^{\{d+1-k\}}\right), \text{ for } 0 \le k \le d.$$

This means that any point of $V$ can be expressed as $\sum_{k=1}^{d} \alpha_k \vec{u}_k$, with $\alpha_k \in \mathbb{Z}$ for all $k \in \{1, \dots, d\}$.

Each coordinate of $(d+1)\vec{u}_k$ is an integer congruent to $k$ modulo $(d+1)$. Following the definition of [1], we call a point a *remainder-k point* if its coordinates are congruent to $k$ modulo $(d+1)$. Since any lattice point $z$ in $V$ can be written as $z = \sum \alpha_k \vec{u}_k$, it follows that $z$ is a $\tilde{k}$-remainder point, where $\tilde{k}$ is congruent to $(\sum \alpha_k \cdot k)$ modulo $(d+1)$.

We will now look at the circumcentre $c = \frac{1}{d+1}\left(-\frac{d}{2}, -\frac{d-2}{2}, -\frac{d-4}{2}, \dots, \frac{d}{2}\right)$ of $\sigma$ and find its nearest neighbours in the lattice. Take $z = \frac{1}{d+1}\left(n_1(d+1)+\tilde{k}, \cdots, n_{d+1}(d+1)+\tilde{k}\right)$ a remainder-$\tilde{k}$ lattice point, for some $\tilde{k} \in \{0, \dots, d\}$.

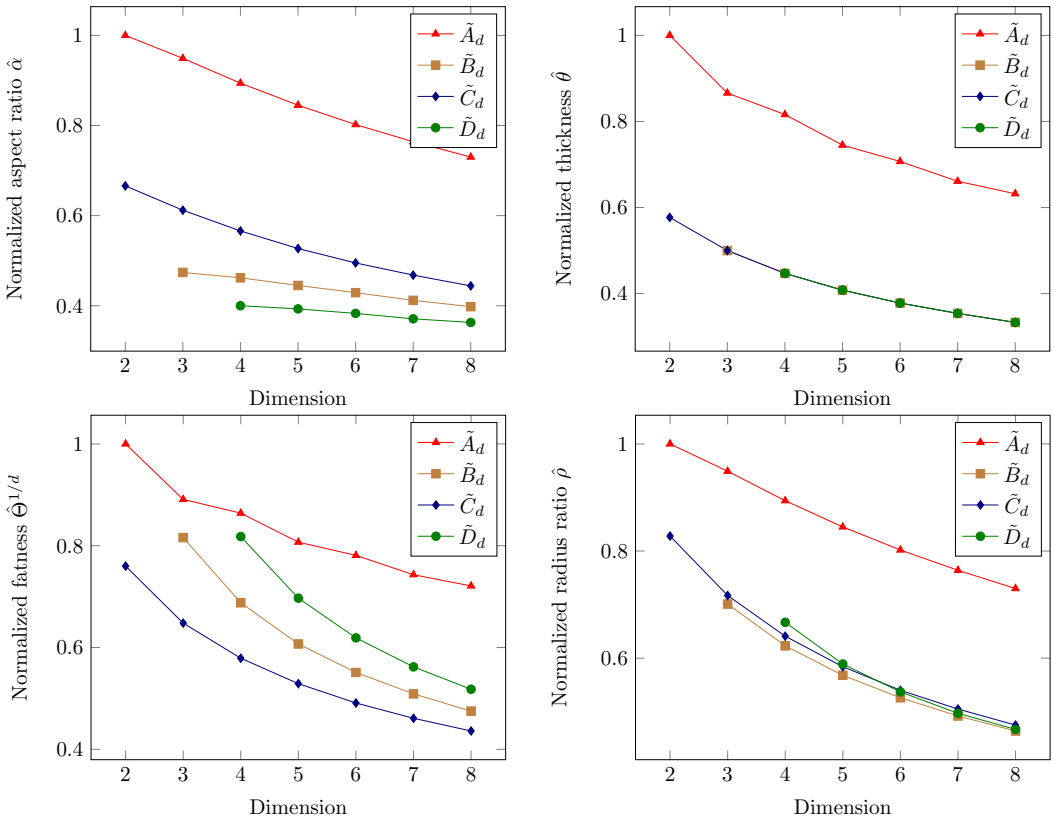


Figure 4: The visual representation of the normalized aspect ratio value, thickness, fatness and the radius ratio for simplices of $\tilde{A}_d$, $\tilde{B}_d$, $\tilde{C}_d$ and $\tilde{D}_d$ triangulations.

Note that because the lattice $V$ resides in the hyperplane $\sum_{i=1}^{d+1} x_i = 0$, we have $\langle z, (1^{\{d+1\}})\rangle = 0$, and therefore $\sum n_i = -\tilde{k}$. We now need to find the value of $n = (n_1, \cdots, n_{d+1}) \in N = \left\{x \in \mathbb{Z}^{d+1} \middle| \sum x_i = -\tilde{k}\right\}$ which minimizes $d(z, c)$ for a given $\tilde{k}$.

We now state the following claim, which will be proved below.

**Claim.** *For each $k \in \mathbb{Z}/(d+1)\mathbb{Z}$, the closest remainder-$k$ point in $V$ to $c$ is $u_k$. A remainder-$k$ point that is the second closest corresponds to the vector $n$ equal to*

$$\begin{cases} (-1^{\{k-1\}}, 0, -1, 0^{\{d-k\}}), & \text{for } k \in \{1, ..., d\} \\ (-1, 0^{\{d-1\}}, 1), & \text{if } k = 0 \end{cases}$$

*and has the coordinates*

$$\begin{cases} ((k-(d+1))^{\{k-1\}}, k, k-(d+1), k^{\{d-k\}}), & \text{for } k \in \{1, ..., d\} \\ (-(d+1), 0^{\{d-1\}}, d+1), & \text{if } k = 0 \end{cases}.$$

*Each of these points are at a distance*

$$R' = \sqrt{\frac{d(d+2)}{12(d+1)} + \frac{2}{d+1}}$$

*from $c$.*

This claim implies that the protection radius of $\sigma$ is

$$R' - R = \sqrt{\frac{d(d+2)}{12(d+1)} + \frac{2}{d+1}} - \sqrt{\frac{d(d+2)}{12(d+1)}}.$$

Thus, the relative protection is

$$\hat{\delta} = \frac{\sqrt{d^2+2d+24} - \sqrt{d^2+2d}}{\sqrt{d^2+2d}} = \sqrt{1 + \frac{24}{d^2+2d}} - 1 \sim \left(1 + \frac{12}{d^2+2d}\right) - 1 \sim \frac{12}{d^2}.$$

This completes the proof of Lemma 6.1 apart from the claim, which we will focus on now. □

The main ingredient for the proof of the Claim is the following lemma.

**Lemma 6.2.** *The difference between the two squared distances $d(z,c)^2$ and $d(z',c)^2$ for two points $z$ and $z'$ of the lattice $V$ is of the form $\frac{2q}{d+1}$ where $q$ is an integer.*

*Proof.* It is enough to compare the distances for $z$ and $z'$ of the same congruence class. Indeed, each congruence class $k$ already contains the point $u_k$, which is of squared distance $R^2$ from $c$. The difference between any two squared distances $d(z,c)^2$ and $d(z',c)^2$, for $z$ and $z'$ a remainder-$k$ and a remainder-$k'$ point respectively, can be expressed as

$$d(z,c)^2 - d(z',c)^2 = (d(z,c)^2 - d(z,u_k)^2) - (d(z',c)^2 - d(z',u_{k'})'^2).$$

If both differences are in $\frac{2}{d+1}\mathbb{Z}$, the overall difference is as well.

So let

$$\begin{aligned} z &= \frac{1}{d+1}\big(n_0(d+1)+k, \cdots, n_d(d+1)+k\big) \text{ and} \\ z' &= \frac{1}{d+1}\big(n'_0(d+1)+k, \cdots, n'_d(d+1)+k\big) \end{aligned}$$

be two remainder-$k$ points of $V$, with $n_i$ and $n'_i$ integers for all $i \in \{1,\ldots,d+1\}$. The difference between $d(z,c)^2$ and $d(z',c)^2$ can be expressed as:

$$\begin{aligned} d(z,c)^2 - d(z',c)^2 &= (\|z\|^2 - 2\langle z,c\rangle + \|c\|^2) - (\|z'\|^2 - 2\langle z',c\rangle + \|c\|^2) \\ &= \|z\|^2 - \|z'\|^2 - 2\langle z-z',c\rangle \\ &= \sum_{i=0}^{d}\left(n_i + \frac{k}{d+1}\right)^2 - \sum_{i=0}^{d}\left(n'_i + \frac{k}{d+1}\right)^2 \\ &\quad -2\sum_{i=0}^{d}\left(n_i + \frac{k}{d+1} - n'_i - \frac{k}{d+1}\right)\left(-\frac{d}{2(d+1)} + \frac{i}{d+1}\right) \\ &= \sum_{i=0}^{d}(n_i - n'_i)\left(n_i + n'_i + \frac{2k}{d+1}\right) + 2\sum_{i=0}^{d}(n_i - n'_i)\left(\frac{d/2-i}{d+1}\right) \\ &= \sum_{i=0}^{d}(n_i - n'_i)\left(n_i + n'_i + \frac{2k+d-2i}{d+1}\right) \end{aligned}$$

Because $\sum_{i=0}^{d} n_i = -k$, we can express $n_0 = -k - \sum_{i=1}^{d} n_i$. Therefore

$$\begin{aligned} d(z,c)^2 - d(z',c)^2 &= \sum_{i=1}^{d}(n_i - n'_i)\left(n_i + n'_i + \frac{2k+d-2i}{d+1}\right) \\ &\quad +(n_0 - n'_0)\left(n_0 + n'_0 + \frac{2k+d}{d+1}\right) \\ &= \sum_{i=1}^{d}(n_i - n'_i)\left(n_i + n'_i + \frac{2k+d-2i}{d+1}\right) \\ &\quad -\left(\sum_{i=1}^{d}(n_i - n'_i)\right)\left(-2k - \sum_{i=1}^{d}(n_i + n'_i) + \frac{2k+d}{d+1}\right) \end{aligned}$$

The last expression is further simplified to

$$\sum_{i=1}^{d}(n_i - n'_i)\left(n_i + n'_i + 2k + \sum_{j=1}^{d}(n_j + n'_j) - \frac{2i}{d+1}\right).$$

We will split this expression in two parts:

$$\sum_{i=1}^{d}(n_i - n'_i)\left(n_i + n'_i + \sum_{j=1}^{d}(n_j + n'_j)\right) + \frac{2}{d+1}\sum_{i=1}^{d}(n_i - n'_i)((d+1)k - i). \tag{1}$$

The second part of the expression (1) is already of the form $\frac{2q'}{d+1}$ with $q'$ an integer, so we will be interested in the first part.

Let $a_i \in \mathbb{Z}/2\mathbb{Z}$ be the congruence class of $(n_i - n_i')$ modulo 2. At the same time, $a_i$ is the congruence class of $(n_i + n_i')$ modulo 2. So the first part of the expression has the congruence class modulo 2 as follows:

$$\sum_{i=1}^{d} a_i \left( a_i + \sum_{j=1}^{d} a_j \right) = \sum_{i=1}^{d} a_i^2 + \left( \sum_{i=1}^{d} a_i \right)^2 = 2 \sum_{i=1}^{d} \sum_{\substack{j=0 \\ j \neq i}}^{d} a_i a_j = 0.$$

It implies that the first part of (1) is an even integer and it can be represented as $\frac{2q''}{d+1}$ for some integer $q''$. Thus, the difference $d(z,c)^2 - d(z',c)^2$ can be expressed as $\frac{2q}{d+1}$ for some integer $q$. □

*Proof (of Claim).* A consequence of Lemma 6.2 is that the minimal positive difference between two squared distances is $\frac{2}{d+1}$. By Theorem 4.9 we know that the triangulation has a non-zero protection, so out of all points in $V$ only the vertices of $\sigma$ are distant from $c$ by the circumradius $R$, and they are unique to be so in their respective congruence class. The squared distance $R'^2$ between the points in the statement of the Claim and the circumcenter $c$ is exactly different from $R^2$ by $\frac{2}{d+1}$, so these points are indeed second closest points to $c$ after the vertices of $\sigma$, which concludes the proofs of the Claim and Lemma 6.1.

□

**Remark 6.3.** *One can verify that the points in the statement of the Claim are the only second closest points to $c$ in $V$, but it goes beyond the scope of this paper.*

# Acknowledgements

The research leading to these results has received funding from the European Research Council (ERC) under the European Union's Seventh Framework Programme (FP/2007-2013) / ERC Grant Agreement No. 339025 GUDHI (Algorithmic Foundations of Geometry Understanding in Higher Dimensions).

We also thank Arijit Ghosh, Ramsay Dyer and Jean-Daniel Boissonnat for discussion and suggestions.

# References

[1] Andrew Adams, Jongmin Baek, and Myers Abraham Davis. Fast High-Dimensional Filtering Using the Permutohedral Lattice. In *Computer Graphics Forum*, volume 29, pages 753–762. Wiley Online Library, 2010.

[2] Ivo Babuška and A Kadir Aziz. On the angle condition in the finite element method. *SIAM Journal on Numerical Analysis*, 13(2):214–226, 1976.

[3] Mikhail Bogdanov, Monique Teillaud, and Gert Vegter. Delaunay triangulations on orientable surfaces of low genus. In *Proceedings of the Thirty-second International Symposium on Computational Geometry*, pages 20:1–20:17, 2016. URL: `https://hal.inria.fr/hal-01276386`, `doi:10.4230/LIPIcs.SoCG.2016.20`.

[4] Jean-Daniel Boissonnat, Ramsay Dyer, and Arijit Ghosh. The stability of Delaunay Triangulations. *Int. J. Comput. Geometry Appl.*, 23(4-5):303–334, 2013. URL: `http://dx.doi.org/10.1142/S0218195913600078`, `doi:10.1142/S0218195913600078`.

[5] Jean-Daniel Boissonnat, Ramsay Dyer, and Arijit Ghosh. Delaunay stability via perturbations. *International Journal of Computational Geometry & Applications*, 24(02):125–152, 2014.

[6] Jean-Daniel Boissonnat, Ramsay Dyer, and Arijit Ghosh. A Probabilistic Approach to Reducing Algebraic Complexity of Delaunay Triangulations. In *Algorithms - ESA 2015 - 23rd Annual European Symposium, Patras, Greece, September 14-16, 2015, Proceedings*, pages 595–606, 2015. URL: `http://dx.doi.org/10.1007/978-3-662-48350-3_50`, `doi:10.1007/978-3-662-48350-3_50`.

[7] Nicolas Bourbaki. Lie groups and Lie algebras. Chapters 4–6. Translated from the 1968 French original by Andrew Pressley. Elements of Mathematics, 2002.

[8] James C. Cavendish, David A. Field, and William H. Frey. An apporach to automatic three-dimensional finite element mesh generation. *International Journal for Numerical Methods in Engineering*, 21(2):329–347, 1985. URL: `http://dx.doi.org/10.1002/nme.1620210210`, `doi:10.1002/nme.1620210210`.

[9] Siu-Wing Cheng, Tamal K Dey, and Edgar A Ramos. Manifold reconstruction from point samples. In *SODA*, volume 5, pages 1018–1027, 2005.

[10] Siu-Wing Cheng, Tamal K Dey, and Jonathan Shewchuk. *Delaunay mesh generation*. CRC Press, 2012.

[11] A. Choudhary, M. Kerber, and S. Raghvendra. Polynomial-sized Topological Approximations using the Permutahedron. *Discrete & Computational Geometry*, Nov 2017.

[12] J. H. Conway and N. J. A. Sloane. *Sphere-packings, Lattices, and Groups*. Springer-Verlag New York, Inc., New York, NY, USA, 1987.

[13] J. H. Conway, N. J. A. Sloane, and E. Bannai. *Sphere-packings, Lattices, and Groups*. Springer-Verlag, 1987.

[14] Harold SM Coxeter. Discrete groups generated by reflections. *Annals of Mathematics*, pages 588–621, 1934.

[15] Ludwig Danzer, Branko Grünbaum, and Victor Klee. Helly's theorem and its relatives. 1963.

[16] David P Dobkin, Allan R Wilks, Silvio VF Levy, and William P Thurston. Contour tracing by piecewise linear approximations. *ACM Transactions on Graphics (TOG)*, 9(4):389–423, 1990.

[17] David A Field and Warren D Smith. Graded tetrahedral finite element meshes. *International Journal for Numerical Methods in Engineering*, 31(3):413–425, 1991.

[18] James E Humphreys. *Reflection groups and Coxeter groups*, volume 29. Cambridge university press, 1992.

[19] Iordan Iordanov and Monique Teillaud. Implementing Delaunay triangulations of the Bolza surface. In *Proceedings of the Thirty-third International Symposium on Computational Geometry*, pages 44:1–44:15, 2017. URL: `https://hal.inria.fr/hal-01568002`, `doi:10.4230/LIPIcs.SoCG.2017.44`.

[20] Pierre Jamet. Estimations d'erreur pour des éléments finis droits presque dégénérés. *Revue française d'automatique, informatique, recherche opérationnelle. Analyse numérique*, 10(1):43–60, 1976.

[21] H. Jung. Über die kleinste Kugel, die eine räumliche Figur einschliesst. *Journal reine angewandte Mathematik*, 123:241–257, 1901.

[22] MS Klamkin. Inequality for a simplex. *SIAM Review*, 27(4):576, 1985.

[23] Michal Křížek. On the maximum angle condition for linear tetrahedral elements. *SIAM Journal on Numerical Analysis*, 29(2):513–520, 1992.

[24] François Labelle and Jonathan Richard Shewchuk. Isosurface stuffing: fast tetrahedral meshes with good dihedral angles. In *ACM Transactions on Graphics (TOG)*, volume 26, page 57. ACM, 2007.

[25] Robert V Moody and Jiří Patera. Voronoi and Delaunay cells of root lattices: classification of their faces and facets by Coxeter-Dynkin diagrams. *Journal of Physics A: Mathematical and General*, 25(19):5089, 1992.

[26] James R Munkres. *Elementary differential topology*, volume 54. Princeton University Press, 1966.

[27] David J Naylor. Filling space with tetrahedra. *International Journal for Numerical Methods in Engineering*, 44(10):1383–1395, 1999.

[28] VT Rajan. Optimality of the Delaunay triangulation in $\mathbb{R}^d$. *Discrete & Computational Geometry*, 12(2):189–202, 1994.

[29] DMY Sommerville. Space-filling tetrahedra in Euclidean space. *Proceedings of the Edinburgh Mathematical Society*, 41:49–57, 1922.

[30] John Lighton Synge. *The hypercircle in mathematical physics*. CUP Archive, 1957.

[31] Thomas Theußl, Torsten Moller, and Meister Eduard Groller. Optimal regular volume sampling. In *Visualization, 2001. VIS'01. Proceedings*, pages 91–546. IEEE, 2001.

[32] Jaap Top. Dynkin diagrammen en Wortelsystemen. URL: `www.math.rug.nl/~top/dynkin.ps`.

[33] Graham M Treece, Richard W Prager, and Andrew H Gee. Regularised marching tetrahedra: improved iso-surface extraction. *Computers & Graphics*, 23(4):583–598, 1999.

[34] Stephen A Vavasis. Stable finite elements for problems with wild coefficients. *SIAM journal on numerical analysis*, 33(3):890–916, 1996.

[35] Hassler Whitney. *Geometric integration theory*. Courier Corporation, 2012.

# A Roots, Groups and lattices: general background

The Coxeter triangulations we use originate in group theoretical studies of symmetries. This section provides a group-theoretical background for and gives a brief introduction of Coxeter triangulations. The first four subsections of the background form a summary of the lecture notes by Jaap Top [32], while the latter subsections give some essential results from Humphreys [18].

## A.1 Graphs and Cartan matrices

We consider undirected connected graphs without loops with $d$ vertices $\{v_1, \ldots, v_d\}$. One can associate an incidence matrix to any such graph, $A = (a_{ij})$. This is the symmetric $d \times d$-matrix with $a_{ij} = 1$ if there is an edge between $v_i$ and $v_j$ and $a_{ij} = 0$ otherwise.

**Definition A.1.** *The Cartan matrix of a graph $\Sigma$ with incidence matrix $A$ is defined by $C = 2I - A$, where $I$ is the identity matrix.*

To each $d \times d$ Cartan matrix we can associate a symmetric bi-linear form $\langle \cdot, \cdot \rangle_C$ on $\mathbb{R}^d$ defined by $\langle u, v \rangle_C = u^t C v$, with $u, v \in \mathbb{R}^d$ and where $u^t$ denotes the transposition of $u$.

We are now interested in identifying the graphs for which the symmetric bi-linear form is positive definite and therefore defines an inner product. Each such $d \times d$ Cartan matrix gives us $d$ linear maps $\sigma_i$, one for each vector $e_i$ of the canonical basis, defined by

$$\begin{array}{rccl} \sigma_i : & \mathbb{R}^d & \to \mathbb{R}^d \\ & x & \mapsto x - \langle x, e_i \rangle_C \, e_i = x - (x^t C e_i) e_i. \end{array}$$

If the bi-linear form $\langle \cdot, \cdot \rangle_C$ is positive definite, the linear map $\sigma_i$ is the orthogonal reflection through the hyperplane, which is orthogonal to $e_i$ with respect to the inner product determined by $C$.

**Definition A.2.** *The Weyl group $W_\Sigma$ of a graph $\Sigma$ is the subgroup of $GL(d, \mathbb{R})$ generated by all $\sigma_i$.*
*The roots of $\Sigma$ are the vectors in the set*

$$R_\Sigma = \{\sigma(e_i) \mid 1 \leq i \leq d, \sigma \in W_\Sigma\}.$$

We now have the following (cf. Section 2.2 of [18]):

**Lemma A.3.** *Let $\Sigma$ be a connected graph with Cartan matrix $C$ and Weyl group $W_\Sigma$.*

- *If $\langle \cdot, \cdot \rangle_C$ is positive definite, that is it defines an inner product, then the action of $W_\Sigma$ on $\mathbb{R}^d$ is irreducible, which means that there is no non-trivial subspace of $\mathbb{R}^d$ (a subspace that is not equal to $\mathbb{R}^d$ or $\{0\}$) that is mapped to itself under the action of $W_\Sigma$.*
- *If $W_\Sigma$ is finite, then the action of $W_\Sigma$ on $\mathbb{R}^d$ is irreducible.*

**Theorem A.4** ([18, Section 1.3])**.** *For a graph $\Sigma$ with Cartan matrix $C$, Weyl group $W_\Sigma$ and root set $R_\Sigma$, the following three statements are equivalent:*

- *$\langle \cdot, \cdot \rangle_C$ is positive definite, that is it defines an inner product.*
- *The root set $R_\Sigma$ is finite.*
- *The Weyl group $W_\Sigma$ is finite.*

The Section 1.8 of [18] also gives us the following proposition:

**Proposition A.5.** *For any graph $\Sigma$ with a positive definite inner product, the action of elements of Weyl group $W_\Sigma$ is simply transitive on the root set $R_\Sigma$.*

The connected graphs $\Sigma$ that give a positive definite form $\langle \cdot, \cdot \rangle_C$ have been classified to be the following (see Section 2.4 of [18]):

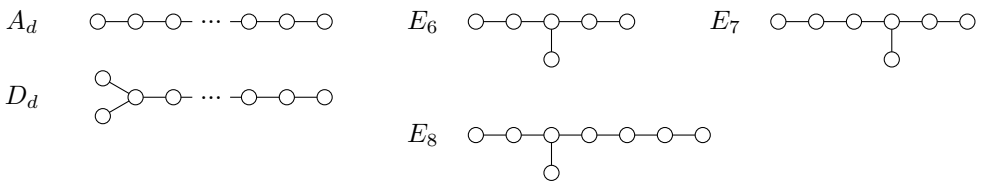


These graphs are called the *Coxeter diagrams* of type $A_d$, $D_d$, $E_6$, $E_7$ and $E_8$. The definition of Coxeter diagrams will be given in Definition A.10.

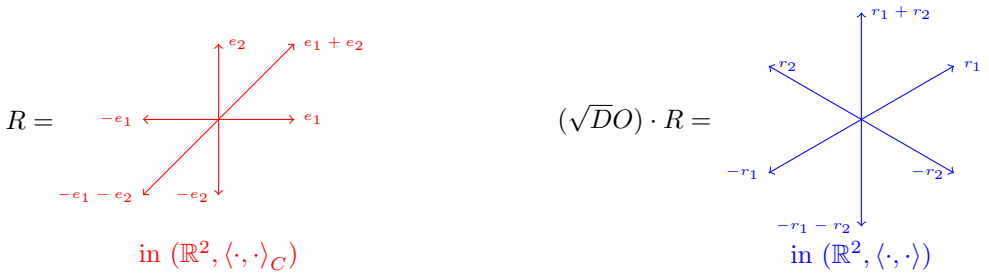


Figure 5: An example of the root sets of the $A_2$ diagram before and after multiplying by $\sqrt{D}O$.

## A.2 Construction of root systems for positive definite graphs

We now want to make the Weyl groups as concrete as possible. To do this we need to find vectors $r_1, \dots r_d \in \mathbb{R}^m$, for $m \geq d$, and $\mathbb{R}^m$ endowed with the standard inner product $\langle\cdot,\cdot\rangle$, such that $\langle r_i, r_j\rangle = c_{ij}$. These vectors are linearly independent because the Cartan matrix $C$ is invertible. In general such a matrix of inner products in called a *Gram* matrix. The span of the vectors $r_i$ will be denoted by $V$.

Note that it is always possible to find such vectors $r_i$, even in $\mathbb{R}^d$. The reason for this is that $C$ can be diagonalized by an orthogonal matrix $O$, $O^t D O = C$. Let us write $D = (d_{ij})$, with $d_{ij} = 0$, if $i \neq j$. If $\sqrt{D}$ denotes the matrix with $\sqrt{d_{ii}}$ on the diagonal, $r_i$ can be found as the $i$th column of the matrix $\sqrt{D}O$ (see Figure 5). Note that this choice is not unique. However in the context of root systems, nicer roots can be chosen, if we allow the roots to lie in $\mathbb{R}^m$ for $m > d$. According to Humphreys[18, Section 2.10], the nice choices are not so obvious, and historically arose from close scrutiny of simple Lie algebras.

The linear maps $\varphi_i$ given by $\varphi_i(v) = v - \langle v, r_i\rangle_C\, r_i$, are automorphisms of $V$ and their matrices with respect to the basis $\{r_1, \dots, r_d\}$ coincide with the matrices of the generators $\sigma_i$ of the Weyl group. This means we can identify all roots with images of $r_i$ under products of $\varphi_j$s, and the Weyl group may be identified with the group generated by the $\varphi_j$s.

The vectors for graphs $\Sigma$ that give a positive definite form $\langle\cdot,\cdot\rangle_C$ are listed in Theorem A.12.

## A.3 Root systems

As we have seen in the previous section, a root set $R$ of each of the diagrams $A_d$, $D_d$, $E_6$, $E_7$ and $E_8$ is stable under the reflections of its roots. These reflections therefore generate a finite group. We will now construct more of such groups based on finite sets of $\mathbb{R}^d$ and properties that are similar to the properties of the roots we discussed.

### A.3.1 Definition and properties

We work in $\mathbb{R}^d$ endowed with the standard inner product $\langle\cdot,\cdot\rangle$. For $r \in \mathbb{R}^d$, with $r \neq 0$, the reflection $\sigma_r$ in the hyperplane $\{v \in \mathbb{R}^d \,|\, \langle v, r\rangle = 0\}$ is given by

$$\sigma_r(x) = x - 2\frac{\langle x, r\rangle}{\langle r, r\rangle} r.$$

**Definition A.6.** *A reduced (red) and irreducible (irr) root system in $\mathbb{R}^d$ is a finite set $R \subset \mathbb{R}^d$ that satisfies:*

*(R1)* $0 \notin R$ *and* $R$ *contains a basis of* $\mathbb{R}^d$

*(R2) For all* $r \in R$, $\sigma_r(R) \subset R$

*(R3) For all* $r, s \in R$, $\sigma_r(s) - s$ *is an integer multiple of* $r$.

*(red) If* $r \in R$ *and* $\lambda r \in R$, *then* $\lambda = \pm 1$

*(irr) There is no decomposition* $R = R_1 \cup R_2$ *with* $R_1 \neq \emptyset \neq R_2$ *and* $\langle r_1, r_2\rangle = 0$ *for all* $r_1 \in R_1$ *and* $r_2 \in R_2$.

*The Weyl groups of the root system $R$ is the (finite) group $W$ generated by the reflections $\sigma_r$.*

From this point onward we shall assume that every root system is reduced and irreducible.

**Remark A.7.** *The angle $\varphi$, with $0 \leq \varphi \leq \pi$, between the two roots $r$, $s$ is given by* $\cos\varphi = \frac{\langle r,s\rangle}{|r||s|}$ . *Note that, due to (R3),*

$$\sigma_r(s) - s = 2\frac{\langle r, s\rangle}{\langle r, r\rangle} r \in \mathbb{Z} \cdot r,$$

*and thus*

$$n(s,r) := 2\frac{\langle r,s\rangle}{\langle r,r\rangle} \in \mathbb{Z}.$$

*It follows that* $4\cos^2\varphi = n(s,r)\cdot n(r,s) \in \mathbb{Z}$. *In the case* $\langle r,s\rangle \neq 0$, *observe that the ratio of the squared norms of these two roots is given by* $\frac{\langle s,s\rangle}{\langle r,r\rangle} = \frac{2\langle r,s\rangle}{\langle r,r\rangle}\frac{\langle s,s\rangle}{2\langle r,s\rangle} = \frac{n(s,r)}{n(r,s)}$. *This gives us, up to symmetry, the following table:*

| $4\cos^2\varphi$ | $n(s,r)$ | $n(r,s)$ | $\varphi$ | *length relation* | *order*$(\sigma_r\sigma_s)$ |
|---|---|---|---|---|---|
| 4 | 2 | 2 | 0 | $r = s$ | 1 |
| 4 | $-2$ | $-2$ | $\pi$ | $r = -s$ | 1 |
| 3 | 3 | 1 | $\pi/6$ | $\lvert s\rvert = \sqrt{3}\lvert r\rvert$ | 6 |
| 3 | $-3$ | $-1$ | $5\pi/6$ | $\lvert s\rvert = \sqrt{3}\lvert r\rvert$ | 6 |
| 2 | 2 | 1 | $\pi/4$ | $\lvert s\rvert = \sqrt{2}\lvert r\rvert$ | 4 |
| 2 | $-2$ | $-1$ | $3\pi/4$ | $\lvert s\rvert = \sqrt{2}\lvert r\rvert$ | 4 |
| 1 | 1 | 1 | $\pi/3$ | $\lvert s\rvert = \lvert r\rvert$ | 3 |
| 1 | $-1$ | $-1$ | $2\pi/3$ | $\lvert s\rvert = \lvert r\rvert$ | 3 |
| 0 | 0 | 0 | $\pi/2$ | *(undetermined)* | 2 |

*By inspection of the table we observe that the length ratio of any two roots can only be* 1, $\sqrt{2}$ *or* $\sqrt{3}$. *It implies that there are at most two different norms of roots, and in this case we speak about* short *and* long *roots.*

**Definition A.8.** *Assume that for a root system* $R$ *we are given an arbitrary* $t \in \mathbb{R}^d$ *such that* $\langle t,r\rangle \neq 0$ *for all* $r \in R$. *The root system now decomposes as* $R = R_t^+ \cup R_t^-$ *into* positive roots $R_t^+ = \{r \in R \mid \langle r,t\rangle > 0\}$ *and* negative roots $R_t^- = \{r \in R \mid \langle r,t\rangle < 0\}$. *A root* $r \in R_t^+$ *is called* decomposable *if* $r = r_1 + r_2$, *with* $r_1, r_2 \in R_t^+$, *and a root* $r \in R_t^+$ *is called simple if it is not decomposable. The set of simple roots is denoted by* $S_t$.

**Lemma A.9.** *For any two simple roots* $r \neq s$ *we have:*

- $\langle r,s\rangle \leq 0$.
- *The simple roots form a basis of* $\mathbb{R}^d$.
- *The Weyl group is generated by the reflections associated to the simple roots.*

We refer to Sections 1.3 and 1.5 of Humphreys [18] for the proof of the lemma.

Because $n(r,s) \in \{-3,-2,-1,0\}$ and $n(s,r)\cdot n(r,s) = 4\cos^2\varphi$, the angle $\varphi$ between $r$ and $s$ equals $\frac{\pi}{2}$, $\frac{2\pi}{3}$, $\frac{3\pi}{4}$ or $\frac{5\pi}{6}$. This information can be represented in a graph.

**Definition A.10.** *Given a root system* $R$ *and a set of simple roots* $S_t$. *We can assume without loss of generality that the short roots in* $S_t$ *have length* 1, *because we can always rescale all roots.*
*The* Coxeter diagram *of* $R$ *consists of a graph with the following data: For each* $r \in S_t$ *we insert one vertex. For every pair* $r \neq s$ *in* $S_t$ *with* $\langle r,s\rangle \neq 0$ *we define a number* $m(r,s) \in \{2,3,4,6\}$, *such that* $\frac{\pi}{m(r,s)} = \arccos\lvert\cos\varphi\rvert$, *where* $\varphi$ *is an angle between* $r$ *and* $s$. *We then insert an edge between* $r$ *and* $s$ *and write the number* $m(r,s)$ *next to it.*
*We further follow the convention not to draw an edge labelled* 2 *and not denote the label* 3 *next to an edge.*

Lemma A.9 states that the simple roots $S_t$ form a basis of $\mathbb{R}^d$. So the standard inner product can be expressed in terms of the basis $S_t$. If we write

$$v = \sum_{r\in S_t} v_r r \qquad\qquad w = \sum_{r\in S_t} w_r r$$

we see that

$$\langle v,w\rangle = \sum_{r\in S_t} v_r w_r \langle r,r\rangle + \sum_{r\neq s\in S_t} v_r w_s \langle r,s\rangle .$$

Because the Euclidean inner product is a positive definite form it is positive definite with respect to any basis. To put it differently the right hand side must be positive definite too. The classification of all Coxeter diagrams can now be performed based on the determination which bilinear forms

$$\sum_{r\in S_t} v_r w_r \langle r,r\rangle + \sum_{r\neq s\in S_t} v_r w_s \langle r,s\rangle = \sum_{r\in S_t} v_r w_r \langle r,r\rangle + \frac{1}{2}\sum_{r\neq s\in S_t} v_r w_s \sqrt{\langle r,r\rangle \langle s,s\rangle m(r,s)}$$

are positive definite. After rescaling this reduces to determining for which diagrams the quadratic form

$$\langle r,s\rangle_C = \sum_{r\in S_t} v_r v_r + \frac{1}{2}\sum_{r\neq s\in S_t} v_r v_s \sqrt{m(r,s)}$$

is positive definite. Such a determination yields:

**Theorem A.11.** *The complete list of Coxeter diagrams of reduced and irreducible root systems consists of $A_d$, $D_d$, $E_6$, $E_7$ and $E_8$ and the following diagrams:*

$B_d (= C_d)$ 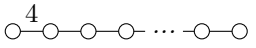

$F_4$ 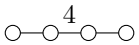

$G_2$ 

*In this list the root system $C_d$ is defined as dual to $B_d$ (see Definition A.15). As a root and a dual root systems they share the same Coxeter diagram and Weyl group (see Section A.4).*

See for example Sections 2.4 and 2.7 of Humphreys [18] for a proof and more information on the classification of Coxeter diagrams.

Having the classification, we can give the roots explicitly as discussed in Section A.2:

**Theorem A.12** ([7])**.** *Let $\{e_1, \ldots, e_d\}$ be the canonical basis in $\mathbb{R}^d$. The complete list of simple root sets (up to scale, rotation and permutation) is the following:*

- $\mathbf{A_d}$ *(in $\mathbb{R}^{d+1}$):* $s_1 = e_1 - e_2$, $s_2 = e_2 - e_3$, $\ldots$, $s_d = e_d - e_{d+1}$.
- $\mathbf{B_d}$*:* $s_1 = e_1 - e_2$, $s_2 = e_2 - e_3$, $\ldots$, $s_{d-1} = e_{d-1} - e_d$, $s_d = e_d$.
- $\mathbf{C_d}$*:* $s_1 = e_1 - e_2$, $s_2 = e_2 - e_3$, $\ldots$, $s_{d-1} = e_{d-1} - e_d$, $s_d = 2e_d$.
- $\mathbf{D_d}$*:* $s_1 = e_1 - e_2$, $s_2 = e_2 - e_3$, $\ldots$, $s_{d-1} = e_{d-1} - e_d$, $s_d = e_{d-1} + e_d$.
- $\mathbf{E_6}$ *(in $\mathbb{R}^8$):* $s_1 = \frac{1}{2}(e_1 + e_8) - \frac{1}{2}(e_2 + e_3 + e_4 + e_5 + e_6 + e_7)$, $s_2 = e_1 + e_2$, $s_3 = e_2 - e_1$, $s_4 = e_3 - e_2$, $s_5 = e_4 - e_3$, $s_6 = e_5 - e_4$.
- $\mathbf{E_7}$ *(in $\mathbb{R}^8$):* $s_1 = \frac{1}{2}(e_1 + e_8) - \frac{1}{2}(e_2 + e_3 + e_4 + e_5 + e_6 + e_7)$, $s_2 = e_1 + e_2$, $s_3 = e_2 - e_1$, $s_4 = e_3 - e_2$, $s_5 = e_4 - e_3$, $s_6 = e_5 - e_4$, $s_7 = e_6 - e_5$.
- $\mathbf{E_8}$*:* $s_1 = \frac{1}{2}(e_1 + e_8) - \frac{1}{2}(e_2 + e_3 + e_4 + e_5 + e_6 + e_7)$, $s_2 = e_1 + e_2$, $s_3 = e_2 - e_1$, $s_4 = e_3 - e_2$, $s_5 = e_4 - e_3$, $s_6 = e_5 - e_4$, $s_7 = e_6 - e_5$, $s_8 = e_7 - e_6$.
- $\mathbf{F_4}$*:* $s_1 = e_2 - e_3$, $s_2 = e_3 - e_4$, $s_3 = e_4$, $s_4 = \frac{1}{2}(e_1 - e_2 - e_3 - e_4)$.
- $\mathbf{G_2}$ *(in $\mathbb{R}^3$):* $s_1 = e_1 - e_2$, $s_2 = -2e_1 + e_2 + e_3$.

*In this list the root system $C_d$ is defined as dual to $B_d$ (see Definition A.15).*

**Remark A.13.** *The list of positive definite graphs also includes the following graphs:*

$H_3$ 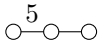

$H_4$ 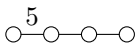

$I_n$ 

*The corresponding reflection groups are the isometry groups of the icosahedron ($H_3$), the isometry group of a regular 120-sided solid with dodecahedral faces in $\mathbb{R}^4$ ($H_4$) and the dihedral group $D_n$ ($I_2(n)$). These diagrams do not correspond to Weyl groups, with the following exceptions: $I_2(6)$, which is traditionally denoted as $G_2$ in the context of Weyl groups, $I_2(3)$ which corresponds to $A_2$ and $I_2(4)$, which corresponds to $B_2$. Apart from these three exceptions these groups violate condition (R3) and are also called non-crystallographic (they do not correspond to locally finite lattices), hence are not considered in this paper. We refer to Humpreys [18, Sections 2.8 and 2.13] for further reading.*

## A.4 Root lattices

We can now define lattices based on the roots we discussed above. These lattices will be essential to the remainder of the text.

**Definition A.14.** *The root lattice $\Lambda_R$ of a root system $R$ is defined as*

$$\Lambda_R = \left\{ \sum_{r \in R} n_r r \mid n_r \in \mathbb{Z} \right\}.$$

It is indeed a lattice in the sense that it is a group under addition of vectors, contains a basis of a $\mathbb{R}^d$ and any bounded region contains only a finite number of elements.

**Definition A.15.** *For each root $r \in R$ define its* dual *root (or* coroot*) to be $r^\vee = \frac{2r}{\langle r,r\rangle}$. The set of dual roots forms a root system [18, Section 2.9] called* dual root system *and is denoted by $R^\vee$.*

Observe that coroots share the same symmetries $\sigma_i$ as the roots. Therefore they generate the same Weyl group $W$. In most cases, the root system $R^\vee$ is identical to $R$ up to scale and rotation; however, the root systems $B_d$ and $C_d$ are dual to each other [18, Section 2.9]. Short roots in a system $R$ of type $B_d$ give rise to long roots in a system $R^\vee$ of type $C_d$ and vice versa.

**Definition A.16.** *Similarly to root lattices, we define a* coroot lattice $\Lambda_{R^\vee}$*:*

$$\Lambda_{R^\vee} = \left\{ \sum_{r\in R} n_r r^\vee \mid n_r \in \mathbb{Z} \right\}.$$

Another important family of lattices is so-called *weight lattices*:

**Definition A.17.** *The set of points which has an integer inner product with all coroots is called the* weight lattice*:*

$$\Lambda_R^w = \left\{ x \in \mathbb{R}^d \mid \langle x, r^\vee\rangle \in \mathbb{Z},\ r \in R \right\}.$$

*Similarly the* coweight lattice *is defined as:*

$$\Lambda_{R^\vee}^w = \left\{ x \in \mathbb{R}^d \mid \langle x, r\rangle \in \mathbb{Z},\ r \in R \right\}.$$

## A.5 Affine reflection groups

The goal for us now is to define a triangulation of the Euclidean space associated to every root system.

First, we need the following definitions:

**Definition A.18** (Affine Weyl group)**.** *Let $R \subset \mathbb{R}^d$ be a finite root system. For every root $r \in R$ and integer $k \in \mathbb{Z}$ we define an affine hyperplane:*

$$H_{r,k} := \{x \in \mathbb{R}^d \mid \langle x, r\rangle = k\}.$$

*The set of affine hyperplanes $H_{r,k}$ for all $r \in R$ and $k \in \mathbb{Z}$ will be denoted as $\mathcal{H}$. To each $H_{r,k}$ we can associate an affine reflection $\sigma_{r,k} : x \mapsto x - (\langle x, r\rangle - k)r^\vee$. These reflections generate a subgroup of the group of affine transformations of $\mathbb{R}^d$, which is called the* affine Weyl group *and is denoted by $W_a$.*

Roughly speaking, the affine Weyl group is a combination of the Weyl group and translations along a lattice. This can be made more precise using the dual lattice $\Lambda_{R^\vee}$ defined in Section A.4:

**Proposition A.19.** *Let $R$ be a root system and $W$ be a corresponding Weyl group. $W_a$ is a semidirect product of $W$ and the translation group corresponding to the coroot lattice $\Lambda_{R^\vee}$.*

We refer to Section 4.2 of [18] for more information.

By Definition A.15, the dual roots are rescaled versions of roots such that the inner product of a root and its dual is 2 (see Figure 7). We can also define these dual roots as follows: one defines $\sigma_{r,k}$ as the affine reflection that leaves $H_{r,k}$ invariant. With this definition the dual root $r^\vee$ is the image of 0 under the reflection $\sigma_{r,1}$. In general, the image of 0 by $\sigma_{r,k}$ is $kr^\vee$ (see Figure 6).

The positions of hyperplanes $H_{r,k}$ with respect to primal and dual root systems in $\mathbb{R}^2$ are illustrated in Figure 7. We notice that the open regions in between the hyperplanes $H_{r,k}$ are congruent triangles. These regions are called alcoves and are the subject of our study in the following. We now formalize:

**Definition A.20.** *Define $\mathcal{A}$ to be the set of connected components of $\mathbb{R}^d \setminus \bigcup_{H\in\mathcal{H}} H$. Each element in $\mathcal{A}$ is called an* alcove*.*

Let $R^+$ be a set of positive roots and $S$ the corresponding simple system. In general, an alcove is characterized by a set of inequalities of the form: $\forall r \in R^+, k_r < \langle x, r\rangle < k_r + 1$, with $k_r$ integers. We will denote by $A^o$ the particular alcove for which all $k_r$ are equal to 0:

$$A^o = \{x \in \mathbb{R}^d \mid \forall r \in R^+, 0 < \langle x, r\rangle < 1\}$$

If the root system $R$ is irreducible, most of the inequalities that define $A^o$ are redundant. If we want to eliminate the redundant inequalities, we first need to define the so called *highest root*.

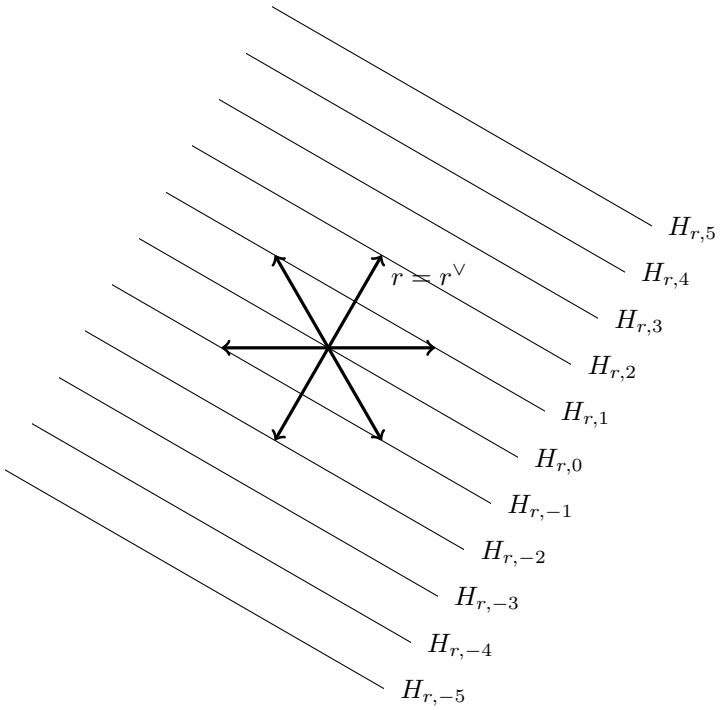


Figure 6: Root system $A_2$ and the hyperplanes $H_{r,k}$ corresponding to the root $r$. Note that $\|r\|^2 = 2$, therefore the primal and the dual roots coincide and the hyperplane $H_{r,1}$ goes halfway through $r = r^\vee$.

Because simple roots $S$ form a basis of the irreducible root system $R$, any root can be decomposed as a sum of simple roots with integer coefficients. So for any two roots $r$ and $r'$ we can write $r = \sum_{i=1}^{d} c_i s_i$ and $r' = \sum_{i=1}^{d} c'_i s_i$, where $S = \{s_1, \ldots, s_d\}$ and the coefficients $c_i$ and $c'_i$ are integers. This gives a partial order $\preccurlyeq$ on the set of roots $R$, which compares the coefficients of two roots meaning that $r \preccurlyeq r'$ if and only if $c_i \leq c'_i$ for all $1 \leq i \leq d$. Using the decomposition, the positive roots $R^+$ can be characterized as the roots that have non-negative coefficients when expressed in terms of simple roots.

**Proposition A.21** (Existence and uniqueness of the highest root)**.** *For an irreducible root system $R$ and a simple root set $S \subset R$, there is a unique maximal element $\tilde{s} \in R^+$ for the partial order $\preccurlyeq$, which is called the highest root.*

**Remark A.22.** *If $R$ has multiple irreducible components there is a highest root for each of them.*

For proofs and more details on the highest root we refer to Section 2.9 of Humphreys [18].

The following proposition states that there are exactly $d+1$ hyperplanes that delimit $A^o$: $d$ hyperplanes corresponding to simple roots and one corresponding to the highest root:

**Proposition A.23** ([18, Section 4.3])**.** *Let $R$ be a root system and $S \subset R$ a set of simple roots. The alcove $A^o$ is an open simplex bounded by $d+1$ hyperplanes. Of them, $d$ hyperplanes are of the form $H_{s,0} = \{x \in \mathbb{R}^d \mid \langle x, s\rangle = 0\}$, one for each simple root $s \in S$ and the final hyperplane is $H_{\tilde{s},1} = \{x \in \mathbb{R}^d \mid \langle x, \tilde{s}\rangle = 1\}$ where $\tilde{s}$ is the highest root.*

Now, we are interested in the closure of the alcove $A^o$. This simplex will be the starting point of the triangulations we will construct.

**Definition A.24.** *Let $R$ be a root system and $S \subset R$ a set of simple roots. Let $A^o$ be the alcove as above. The closure $F$ of $A^o$ is called the* fundamental domain *(or fundamental simplex) of $R$ with respect to $S$.*

**Proposition A.25** ([18, Section 4.3])**.** *Let $R$ be a root system and $S \subset R$ be a set of simple roots. Let $\mathcal{A}$ be the set of alcoves. The affine Weyl group $W_a$ acts simply transitively on $\mathcal{A}$.*

The reason behind the name *fundamental domain* is that the group $W_a$ acts simply transitively on $\mathcal{A}$. In other words, any alcove $A$ is an image of $A^o$ under a unique transformation $w \in W_a$, as the following proposition states.

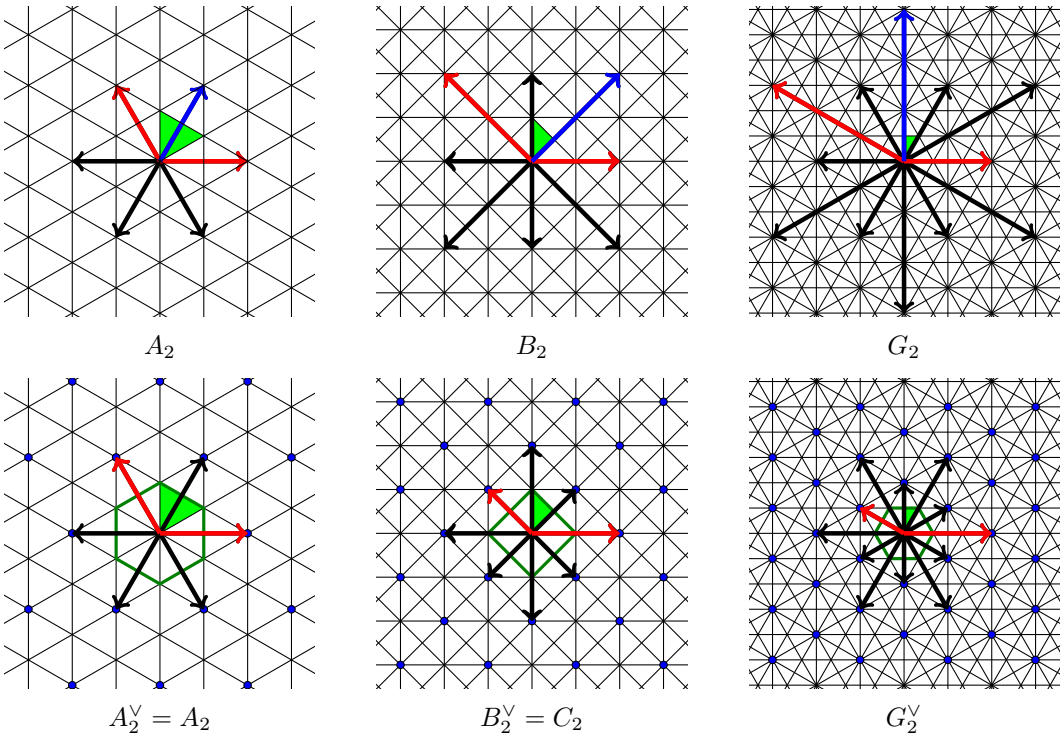


Figure 7: Above: Three root systems and corresponding affine hyperplanes in $\mathbb{R}^2$. Simple roots are marked in red, the highest root in blue and the fundamental domain in green. Each triangle in the background is an alcove. Below: The dual root systems put on the same grid of affine hyperplanes. For the sake of illustrating Proposition A.27, the coroot lattice as well as the Voronoi cell Vor(0) in the Voronoi diagram of the coroot lattice are shown as well.

This means that closures of the elements of $\mathcal{A}$ are all full-dimensional simplices in a triangulation of $\mathbb{R}^d$. By the simple transitivity of the action of $W_a$, all simplices in such a triangulation are congruent to each other, and in particular to the fundamental domain itself.

**Corollary A.26.** *The set $\mathcal{T} = \{\bar{A} \mid A \in \mathcal{A}\}$ gives a triangulation of $\mathbb{R}^d$.*

We call such triangulations *Coxeter triangulations.*

Another more geometric way to get the corollary above is linked with the Voronoi diagram of coroot lattice $\Lambda_{R^\vee}$ (see also Figure 7):

**Proposition A.27** ([13, Chapter 21])**.** *Let $R$ be a root system and $W$ the corresponding Weyl group. Let $F$ be the fundamental domain of $R$ with respect to a set of simple roots $S \subset R$. Then the Voronoi cell of 0 in the Voronoi diagram of the coroot lattice $\Lambda_R$ is:*

$$\mathrm{Vor}(0) \;=\; WF \;:=\; \bigcup_{w \in W} wF$$

Simply put, simplices in $WF$ triangulate the Voronoi cell of 0, even though the term "triangulate the Voronoi cell" although it is somewhat abusive: the vertices of the triangulation we build consists not only of the vertices of the Voronoi cell, but also of its centre.

The *Coxeter diagrams* for Affine Weyl groups are defined in the same way as in Definition A.10, except that we use not only the simple roots, but the highest root as well. This means that the vertices correspond to simple roots and the highest root, and the edges correspond to angles between them.

The classification of all affine Weyl groups is possible thanks to the notion of subgraph and the following lemma:

**Definition A.28.** *A subgraph of a Coxeter diagram $G$ is a Coxeter diagram $G'$ obtained by omitting some vertices (and adjacent edges) of $G'$ or by decreasing the labels on one or more edges.*

**Lemma A.29** ([18, Corollary 2.6])**.** *Every subgraph of an affine Coxeter diagram has a positive definite Cartan matrix.*

Based on these results we can now derive:

**Theorem A.30.** *The complete list of affine Weyl groups and the corresponding Coxeter diagrams is as follows:*

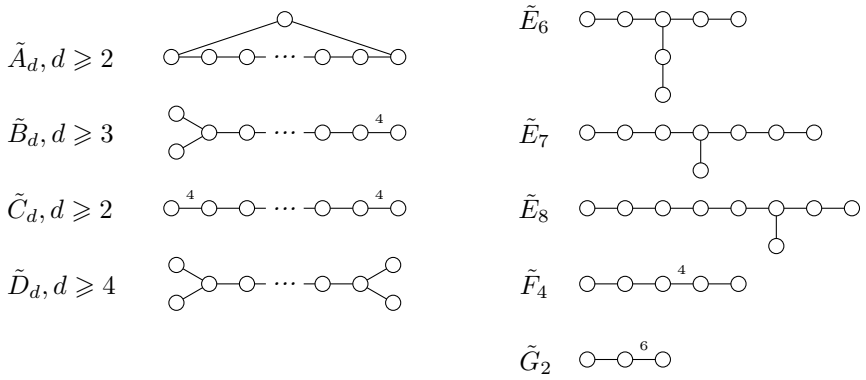


For a proof we refer to Sections 2.5 and 2.7 of [18].

We now have a classification of the Coxeter triangulations, whose properties are the topic of this paper.

# B Geometrical analysis of each family of Coxeter triangulations

For all families we will start with presenting two Coxeter diagrams, an augmented one on the left with coefficients on vertices, which are proportional to inverse heights of a simplex in the triangulation (taken from [16]). The Coxeter diagram on the right indicates the notations of the corresponding facets in the following proofs.

In order to compute the quality measures we will apply the following schema:

1. We give the equations of the hyperplanes containing the facets $\varphi_i$ of a simplex $\sigma$ that generates the root lattice in question.
2. We give the coordinates of the vertices $u_i$ of the simplex $\sigma$.
3. By using the augmented Coxeter diagram we find which height is the shortest (denoted by $h(\sigma)$). We then compute it as the distance from the corresponding vertex to the corresponding hyperplane.
4. We find the circumradius $R(\sigma)$ and the inradius $r(\sigma)$ of the simplex.
5. We find the length of the longest edge $L(\sigma)$, using the coordinates of the vertices found previously.
6. We compute the thickness $\theta(\sigma) = \frac{h(\sigma)}{L(\sigma)}$, the aspect ratio $\alpha(\sigma) = \frac{h(\sigma)}{2R(\sigma)}$ and the radius ratio $\rho(\sigma) = \frac{r(\sigma)}{R(\sigma)}$.
7. We compute the volume $vol(\sigma)$ and the fatness $\Theta(\sigma) = \frac{vol(\sigma)}{L(\sigma)^d}$.
8. We determine if the triangulation is Delaunay with the help of Theorem 4.5. If it is, we also compute its protection value.
9. We determine if the vertex set of the triangulation form a lattice.

The equations for the delimiting hyperplanes of fundamental simplices can be found in [7] or [12], or alternatively can be deduced from Theorem A.12.

We will adopt the following writing convention: the powers in point coordinates correspond to duplications of the same coordinate. For example: $(0, 1^{\{3\}}, 0)$ is the same as $(0, 1, 1, 1, 0)$.

### $\tilde{\mathbf{A}}_\mathbf{d}, \mathbf{d} \geqslant \mathbf{2}$


Figure 8: The augmented Coxeter diagram for the $\tilde{A}_d$ triangulation and the notation of the facets of a corresponding simplex.

| | Fatness $\Theta$ | Aspect Ratio $\alpha$ | Thickness $\theta$ | Radius Ratio $\rho$ |
|---|---|---|---|---|
| $\tilde{A}_d$, $d$ odd | $\frac{2^d}{\left(\sqrt{d+1}\right)^{d+1} d!}$ | $\sqrt{\frac{3(d+1)}{2d(d+2)}}$ | $\sqrt{\frac{2}{d+1}}$ | $\sqrt{\frac{6}{d(d+1)(d+2)}}$ |
| $\tilde{A}_d$, $d$ even | $\frac{2^d(\sqrt{d+1})^{d-1}}{\left(\sqrt{d(d+2)}\right)^{d} d!}$ | | $\sqrt{\frac{2(d+1)}{d(d+2)}}$ | |
| $\tilde{B}_d$ | $\frac{2}{d^{d/2} d!}$ | $\frac{1}{\sqrt{2(d+2)}}$ | $\frac{1}{\sqrt{2d}}$ | $\frac{2}{\sqrt{d+2}(1+(d-1)\sqrt{2})}$ |
| $\tilde{C}_d$ | $\frac{1}{d^{d/2} d!}$ | $\frac{1}{\sqrt{2d}}$ | $\frac{1}{\sqrt{2d}}$ | $\frac{2}{\sqrt{d}(2+(d-1)\sqrt{2})}$ |
| $\tilde{D}_d$ | $\frac{4}{d^{d/2} d!}$ | $\frac{1}{\sqrt{2(d+4)}}$ | $\frac{1}{\sqrt{2d}}$ | $\frac{\sqrt{2}}{\sqrt{d+4}(d-1)}$ |
| $\tilde{E}_6$ | $\frac{\sqrt{3}}{174960}$ | $\frac{1}{6}$ | $\frac{1}{2\sqrt{6}}$ | $\frac{1}{12}$ |
| $\tilde{E}_7$ | $\frac{\sqrt{3}}{14696640}$ | $\frac{1}{2\sqrt{13}}$ | $\frac{1}{4\sqrt{3}}$ | $\frac{2}{9\sqrt{13}}$ |
| $\tilde{E}_8$ | $\frac{1}{696729600}$ | $\frac{1}{2\sqrt{19}}$ | $\frac{1}{6\sqrt{2}}$ | $\frac{1}{5\sqrt{19}}$ |
| $\tilde{F}_4$ | $\frac{1}{576}$ | $\frac{\sqrt{2}}{6}$ | $\frac{\sqrt{2}}{6}$ | $\frac{\sqrt{2}}{3(2+\sqrt{2})}$ |
| $\tilde{G}_2$ | $\frac{\sqrt{3}}{8}$ | $\frac{\sqrt{3}}{4}$ | $\frac{\sqrt{3}}{4}$ | $\frac{1}{1+\sqrt{3}}$ |

Table 2: The non-normalized values for fatness, aspect ratio, thickness and radius ratio of Coxeter triangulations.

1. The delimiting $(d-1)$-planes of the fundamental simplex $\sigma$ in $\mathbb{R}^{d+1}$ can be defined as the intersection of the hyperplane $\sum_{i=0}^{d} x_i = 0$ and the following hyperplanes:
   for $\varphi_0$ : $-x_0 + x_d = 1$
   for $\varphi_k$ : $x_k - x_{k-1} = 0 \quad \forall k \in [\![1, d]\!]$.

2. The vertices of $\sigma$ are (in $\mathbb{R}^{d+1}$):
   $u_0 = \left(0^{\{d+1\}}\right)$
   $u_k = \left((-\frac{d+1-k}{d+1})^{\{k\}}, (\frac{k}{d+1})^{\{d+1-k\}}\right), \quad \forall k \in \{1, \ldots, d\}$.

3. All heights are equal to $h(\sigma) = \frac{1}{\sqrt{2}}$ (see the augmented diagram in Figure 8).

4. The circumcentre coincides with the baricentre $c = \left(-\frac{d}{2(d+1)}, -\frac{d-2}{2(d+1)}, -\frac{d-4}{2(d+1)}, \ldots, \frac{d}{2(d+1)}\right)$ and the circumradius is $R(\sigma) = \sqrt{\frac{d(d+2)}{12(d+1)}}$, which is easily verifiable.
   The incentre coincides with the circumcentre and the inradius is $r(\sigma) = \frac{1}{\sqrt{2}(d+1)}$, which is easily verifiable.

5. The edges of $\sigma$ are described by differences $u_k - u_j$, for certain $j, k \in \{0, \ldots, d\}$ with $j < k$.
   The squared norm of such a difference is equal to $\|\vec{u}_k - \vec{u}_j\|^2 = \frac{(k-j)(d+1-k+j)}{d+1}$.
   An easy analysis (substitute $k - j$ as a new variable) yields that this function on $k$ and $j$ is maximal when $k - j = (d+1)/2$.
   So the maximal edge in $\sigma$ has length $L(\sigma) = \begin{cases} \frac{\sqrt{d+1}}{2} & \text{if } d \text{ is odd} \\ \frac{1}{2}\sqrt{\frac{d(d+2)}{(d+1)}} & \text{if } d \text{ is even} \end{cases}$.

6. The aspect ratio, the thickness and the radius ratio are:
$$\alpha(\sigma) = \sqrt{\frac{3(d+1)}{2d(d+2)}}$$
$$\theta(\sigma) = \begin{cases} \sqrt{\frac{2}{d}} & \text{if } d \text{ is odd} \\ \sqrt{\frac{2(d+1)}{d(d+2)}} & \text{if } d \text{ is even} \end{cases}$$
$$\rho(\sigma) = \sqrt{\frac{6}{d(d+1)(d+2)}}$$

7. **Lemma B.1.** *Simplices in the $\tilde{A}_d$ triangulation have fatness:*
$$\Theta(\sigma) = \begin{cases} \frac{2^d}{\left(\sqrt{d+1}\right)^{d+1} d!} & \textit{if } d \textit{ is odd} \\ \frac{2^d(\sqrt{d+1})^{d-1}}{\left(\sqrt{d(d+2)}\right)^{d} d!} & \textit{if } d \textit{ is even} \end{cases}.$$

The lemma above comes mostly from the fact that the fundamental simplex $\sigma$ has volume:

$$vol(\sigma) = \frac{1}{\sqrt{d+1}\ d!}.$$

*Proof.* Fix the dimension $d \geq 2$. Let $a_k$ denote $-\frac{d+1-k}{d+1}$ and $b_k$ denote $\frac{k}{d+1}$.

Denote by $\sigma$ the $d$-simplex of a $\tilde{A}_d$ triangulation described above. We build a $(d+1)$-simplex $\sigma'$, which consists of the $d$-face $\sigma$ and a vertex $u_{d+1} = (1^{\{d+1\}})$. Note that the edge $u_0 u_{d+1}$ is orthogonal to the face $\sigma$.

The $(d+1)$-dimensional volume of $\sigma'$ can be expressed as a determinant:

$$vol(\sigma') = \left| \frac{1}{(d+1)!} \det \begin{pmatrix} a_1 & a_2 & \dots & a_d & 1 \\ b_1 & a_2 & \dots & a_d & 1 \\ b_1 & b_2 & \dots & a_d & 1 \\ \vdots & \vdots & \ddots & \vdots & \vdots \\ b_1 & b_2 & \dots & b_d & 1 \end{pmatrix} \right|.$$

First, we subtract the last row from all the other rows. It gives us:

$$\begin{aligned} vol(\sigma') &= \left| \frac{1}{(d+1)!} \det \begin{pmatrix} a_1 - b_1 & a_2 - b_2 & \dots & a_d - b_d & 0 \\ 0 & a_2 - b_2 & \dots & a_d - b_d & 0 \\ 0 & 0 & \dots & a_d - b_d & 0 \\ \vdots & \vdots & \ddots & \vdots & \vdots \\ b_1 & b_2 & \dots & b_d & 1 \end{pmatrix} \right| \\ &= \left| \frac{1}{(d+1)!} \det \begin{pmatrix} a_1 - b_1 & a_2 - b_2 & \dots & a_d - b_d \\ 0 & a_2 - b_2 & \dots & a_d - b_d \\ \vdots & \vdots & \ddots & \vdots \\ 0 & 0 & \dots & a_d - b_d \end{pmatrix} \right| \\ &= \left| \frac{1}{(d+1)!} \prod_{k=1}^{d} (a_k - b_k) \right| = \left| \frac{1}{(d+1)!} \prod_{k=1}^{d} \left( -\frac{d+1-k}{d+1} - \frac{k}{d+1} \right) \right| = \frac{1}{(d+1)!}. \end{aligned}$$

The volume of $\sigma$ can be found as:

$$vol(\sigma) = \frac{(d+1)vol(\sigma')}{\|(1^{\{d+1\}})\|} = \frac{(d+1)}{\sqrt{d+1}(d+1)!} = \frac{1}{\sqrt{d+1}\ d!}.$$

□

8. Because the circumcentre coincides with the incentre, it lies inside the simplex. So by Theorem 4.5 the triangulation is Delaunay. It also has a non-zero protection value by Theorem 4.9, the exact value of which is proven in Section 6.

9.

**Proposition B.2.** *The vertex set of a $\tilde{A}_d$ triangulation is a lattice for all $d \geq 2$.*

As we will show, this lattice is in fact the coweight lattice introduced in Section A.4. The fact that the vertex set is a lattice is not entirely obvious. This lattice happens to be equal to the permutahedral lattice studied in for example [12].

Before proving the proposition, we will need the following lemma:

**Lemma B.3.** *Let $R$ be a root system. Let $V$ be the vertex set of the Coxeter triangulation corresponding to $R$. The coweight lattice $\Lambda^w_{R^\vee}$ is a subset of $V$.*

*Proof.* Let $S = \{s_1, \dots, s_d\}$ be a set of simple roots. For any point $p$ in $\Lambda^w_{R^\vee}$ there exist integers $n_1, \dots, n_d$ such that for every $i$, $\langle p, s_i \rangle = n_i$. The point $p$ lies in the intersection of the hyperplanes $H_{s_i,k_i}$. Therefore, being in the intersection of $d$ hyperplanes in $\mathcal{H}$, it is a vertex in the Coxeter triangulation. □

Now, we are ready to prove the proposition.

*Proof.* Take the triangulation generated by $\sigma$ described in the beginning of the section. We will further prove that its vertex set $V$ is the coweight lattice $\Lambda^w_{R^\vee}$ of the root lattice $R$ with the following highest root and simple roots:

$\tilde{s} = (-1, 0^{\{d-1\}}, 1)$
$s_k = (0^{\{k-1\}}, 1, -1, 0^{\{d-k\}})$, for all $k \in \{1, \dots, d\}$.

By Lemma B.3, the coweight lattice $\Lambda^w_{R^\vee}$ is a subset of $V$. Now let us prove the other inclusion.

The highest root can be expressed in terms of the simple roots as: $\tilde{s} = -\sum_{i=1}^{d} s_i$. Because all the coefficients of this decomposition are of absolute value 1, any simple root $s_j$ can be expressed as a sum of the highest root and the rest of the simple roots with integer coefficients: $s_j = \tilde{s} + \sum_{\substack{1 \le i \le d \\ i \neq j}} s_j$.

Let $x$ be a vertex in $V$. The point $x$ lies on $d$ hyperplanes of the form $H_{s,k}$ with $s \in S \cup \{\tilde{s}\}$ and $k \in \mathbb{Z}$. There are two cases to study:

(a) In the first case, all $d$ hyperplanes correspond to simple roots. By the definition of the hyperplanes $H_{s,k}$, this implies that all inner products with the simple roots are integers, which leads to the conclusion that $x$ is in the coweight lattice $\Lambda^w_{R^\vee}$.

(b) In the second case, $d-1$ hyperplanes correspond to simple roots and one hyperplane corresponds to the highest root $\tilde{s}$. Let $s_j$ be the root, whose hyperplane does not appear in the definition of $x$. By definition of $x$, all inner products $\langle x, s_i \rangle$ with $i \neq j$ as well as the inner product $\langle x, \tilde{s} \rangle$ are integers. But then:

$$\langle x, s_j \rangle = \langle x, \tilde{s} \rangle + \sum_{\substack{1 \le i \le d \\ i \neq j}} \langle x, s_j \rangle \in \mathbb{Z}$$

Therefore, all inner products of $x$ with the simple roots are integers, which means that $x$ lies in the coweight lattice $\Lambda^w_{R^\vee}$.

□

**$\tilde{\mathbf{B}}_\mathbf{d}, \mathbf{d} \geqslant \mathbf{3}$**


Figure 9: The augmented Coxeter diagram for the $\tilde{B}_d$ triangulation and the notation of the facets of a corresponding simplex.

1. The delimiting hyperplanes of the fundamental simplex $\sigma$ can be defined as follows:
   $\varphi_0 : \ x_1 + x_2 = 1$
   $\varphi_k : \ x_k - x_{k+1} = 0, \forall k \in \{1, \dots, d-1\}$
   $\varphi_d : \ x_d = 0.$

2. The vertices of $\sigma$ are:
   $u_0 = \left(0^{\{d\}}\right)$
   $u_1 = \left(1, 0^{\{d-1\}}\right)$
   $u_k = \left(\frac{1}{2}^{\{k\}}, 0^{\{d-k\}}\right), \forall k \in \{2, \dots, d\}.$

3. The minimal height falls on any of $\varphi_k$ for $k$ in $\{2, \dots, d-1\}$ and is equal to $h(\sigma) = \frac{1}{2\sqrt{2}}$ (see the augmented diagram in Figure 9).

4. The circumcentre of the simplex is $(\frac{1}{2}, 0, \frac{1}{4}^{\{d-2\}})$ and the circumradius is $R(\sigma) = \frac{\sqrt{d+2}}{4}$, which is easily verifiable. The incentre is $\left(\frac{1+(d-1)\sqrt{2}}{2(1+(d-1)\sqrt{2})}, \frac{1+(d-2)\sqrt{2}}{2(1+(d-1)\sqrt{2})}, \dots, \frac{1}{2(1+(d-1)\sqrt{2})}\right)$ and the inradius is $r(\sigma) = \frac{1}{2(1+(d-1)\sqrt{2})}$, which is easily verifiable.

5. The longest edge is given by $\vec{u}_d - \vec{u}_0$ and is equal to $L(\sigma) = \frac{\sqrt{d}}{2}$.

6. The aspect ratio, the thickness and the radius ratio are:

$$\alpha(\sigma) = \frac{1}{\sqrt{2(d+2)}} \quad \text{and} \quad \theta(\sigma) = \frac{1}{\sqrt{2d}} \quad \text{and} \quad \rho(\sigma) = \frac{2}{\sqrt{d+2}(1+(d-1)\sqrt{2})}$$

7. The volume of the simplex is given by the formula:

$$vol(\sigma) = \frac{1}{d!} \det \begin{pmatrix} 1 & 1/2 & \dots & 1/2 \\ 0 & 1/2 & & 1/2 \\ \vdots & \ddots & \ddots & \vdots \\ 0 & \dots & 0 & 1/2 \end{pmatrix} = \frac{1}{2^{d-1}d!}.$$

The fatness of the simplex is:

$$\Theta(\sigma) = \frac{vol(\sigma)}{L(\sigma)^d} = \frac{2}{d^{d/2}d!}.$$

8. Observe that the inner products of the normal vector $s_2$ to the hyperplane $\varphi_2$ with the circumcentre and $u_2$ have different signs:

$$\langle s_2, c \rangle = -\frac{1}{4} \quad \text{and} \quad \langle s_2, u_2 \rangle = \frac{1}{2}.$$

Therefore the hyperplane $\varphi_2$ separates the circumcentre $c$ from $u_2$, so by Theorem 4.5 the triangulation is not Delaunay.

9. 

**Proposition B.4.** *No vertex set of a $\tilde{B}_d$ triangulation for $d \geq 3$ is a lattice.*

*Proof.* A point $v \in \mathbb{R}^d$ is a vertex of the triangulation if and only if it lies in the intersection of at least $d$ hyperplanes in $\mathcal{H}$ (as defined in Section A.5) that are linearly independent. Equivalently, the inner products of at least $d$ linearly independent positive roots should be integers.

Let $E = \{e_1, ..., e_d\}$ be the canonical base of $\mathbb{R}^d$. Bourbaki [7, Planche II] gives the explicit expressions of positive roots:

$$\begin{aligned} R^+ \quad = \quad & \{e_i \mid i \in \{1, \dots, d\}\} \cup \\ & \{e_i - e_j \mid i, j \in \{1, \dots, d\} \text{ and } i < j\} \cup \\ & \{e_i + e_j \mid i, j \in \{1, \dots, d\} \text{ and } i < j\}. \end{aligned}$$

We will now prove that $v = u_d - u_{d-1} = \frac{1}{2}e_d$ is not in the vertex set, which implies that $V$ does not form a lattice.

The positive roots that have integer inner product with $v$ are exactly:

$$\begin{aligned} & \{e_i \mid i \in \{1, \dots, d-1\}\} \cup \\ & \{e_i - e_j \mid i, j \in \{1, \dots, d-1\} \text{ and } i < j\} \cup \\ & \{e_i + e_j \mid i, j \in \{1, \dots, d-1\} \text{ and } i < j\}, \end{aligned}$$

which is easily verifiable.

These roots span the vector space $\text{Vect}(E \setminus \{e_d\})$, which is $(d-1)$-dimensional. Thus, there do not exist $(r_1, ..., r_d) \subseteq R^+$ that are linearly independent and have integer inner products with $v$. Therefore $v$ does not belong to $V$.

□

### $\tilde{\mathbf{C}}_\mathbf{d}, \mathbf{d} \geqslant \mathbf{2}$


Figure 10: The augmented Coxeter diagram for the $\tilde{C}_d$ triangulation and the notation of the facets of a corresponding simplex.

1. The delimiting hyperplanes of the fundamental simplex $\sigma$ can be defined as follows:

$\varphi_0 : \ 2x_1 = 1$
$\varphi_k : \ x_k - x_{k+1} = 0, \forall k \in \{1, \dots, d-1\}$
$\varphi_d : \ x_d = 0.$

2. The vertices of $\sigma$ are:
   $u_k = \left(\frac{1}{2}^{\{k\}}, 0^{\{d-k\}}\right), \forall k \in \{0, \ldots, d\}$.

3. The minimal height falls on any of $\varphi_k$ for $k$ in $\{1, \ldots, d-1\}$ and is equal to $h(\sigma) = \frac{1}{2\sqrt{2}}$ (see the augmented diagram in Figure 10).

4. The circumcentre of the simplex is $(\frac{1}{4}^{\{d\}})$ and the circumradius is $R(\sigma) = \frac{\sqrt{d}}{4}$, which is easily verifiable. The incentre is $\left(\frac{1+(d-1)\sqrt{2}}{2(2+(d-1)\sqrt{2})}, \frac{1+(d-2)\sqrt{2}}{2(2+(d-1)\sqrt{2})}, \ldots, \frac{1}{2(2+(d-1)\sqrt{2})}\right)$ and the inradius is $r(\sigma) = \frac{1}{2(2+(d-1)\sqrt{2})}$, which is easily verifiable.

5. The longest edge is given by $\vec{u}_d - \vec{u}_0$ and is equal to $L(\sigma) = \frac{\sqrt{d}}{2}$.

6. The aspect ratio, the thickness and the radius ratio are:

$$\alpha(\sigma) = \frac{1}{\sqrt{2d}} \quad \text{and} \quad \theta(\sigma) = \frac{1}{\sqrt{2d}} \quad \text{and} \quad \rho(\sigma) = \frac{2}{\sqrt{d}(2+(d-1)\sqrt{2})}.$$

7. The volume of the simplex is given by the formula:

$$vol(\sigma) = \frac{1}{d!} \det \begin{pmatrix} 1/2 & 1/2 & \ldots & 1/2 \\ 0 & 1/2 & & 1/2 \\ \vdots & \ddots & \ddots & \vdots \\ 0 & \ldots & 0 & 1/2 \end{pmatrix} = \frac{1}{2^d d!}.$$

   The fatness of the simplex is:

$$\Theta(\sigma) = \frac{vol(\sigma)}{L(\sigma)^d} = \frac{1}{d^{d/2} d!}.$$

8. Observe that all inner products of the normals $s_i$ to hyperplanes $\varphi_i$ and the corresponding opposite vertices $u_i$ are positive. Observe as well that the inner products with the circumcentre $\langle s_i, c\rangle$ are either positive or zero. It implies that the circumcentre lies on the boundary of the simplex, therefore by Theorem 4.8 the triangulation is non-protected Delaunay.

9.

**Proposition B.5.** *The vertex set of a $\tilde{C}_d$ triangulation is a lattice for $d \geq 2$.*

*Proof.* A point $v \in \mathbb{R}^d$ is a vertex of the triangulation if and only if it lies in the intersection of at least $d$ hyperplanes in $\mathcal{H}$ (as defined in Section A.5) that are linearly independent. Equivalently, the inner products of at least $d$ linearly independent positive roots should be integers.

Let $E = \{e_1, ..., e_d\}$ be the canonical base of $\mathbb{R}^d$. Bourbaki [7, Planche III] gives the explicit expressions of positive roots:

$$\begin{aligned} R^+ \quad = \quad & \{2e_i \mid i \in \{1, \ldots, d\}\} \cup \\ & \{e_i - e_j \mid i, j \in \{1, \ldots, d\} \text{ and } i < j\} \cup \\ & \{e_i + e_j \mid i, j \in \{1, \ldots, d\} \text{ and } i < j\}. \end{aligned}$$

We will denote by $V$ the vertex set of the $\tilde{C}_d$ triangulation that contains the simplex $\sigma$. The goal is to prove that $V = (\frac{1}{2}\mathbb{Z})^d$, which is a lattice.

We will first prove that $V \subseteq (\frac{1}{2}\mathbb{Z})^d$. Indeed, for any $x \in (\frac{1}{2}\mathbb{Z})^d$, its image by an affine reflection $\sigma_{r,k}$ for $r \in R$ and $k \in \mathbb{Z}$, as defined in Section A.5, is $\sigma_{r,k}(x) = x - (\langle x, r\rangle - k)r^\vee$. For any $r \in R$ and $x \in (\frac{1}{2}\mathbb{Z})^d$, the inner product $\langle x, r\rangle$ is in $\frac{1}{2}\mathbb{Z}$, hence $(\langle x, r\rangle - k)$ is in $\frac{1}{2}\mathbb{Z}$ as well. The dual root $r^\vee$ has integer coefficients, so $\sigma_{r,k}(x) = x - (\langle x, r\rangle - k)r^\vee$ is in $(\frac{1}{2}\mathbb{Z})^d$. Now recall that one can obtain any simplex from another one by a series of affine reflections. All vertices of $\sigma$ are in $(\frac{1}{2}\mathbb{Z})^d$, so with the above observation we conclude that any vertex in $V$ is in $(\frac{1}{2}\mathbb{Z})^d$ as well.

To prove the other direction, observe that $\{2e_i \mid i \in \{1, \ldots, d\}\}$ is a set of $d$ linearly independent positive roots that have integer inner products with any element in $(\frac{1}{2}\mathbb{Z})^d$.

With both inclusions proven, we conclude that $V = (\frac{1}{2}\mathbb{Z})^d$, which is a lattice.

□


Figure 11: The augmented Coxeter diagram for the $\tilde{D}_d$ triangulation and the notation of the facets of a corresponding simplex.

### $\tilde{\mathbf{D}}_\mathbf{d}, \mathbf{d} \geqslant \mathbf{4}$

1. The delimiting hyperplanes of the fundamental simplex $\sigma$ can be defined as follows:
   $\varphi_0 : \ x_1 + x_2 = 1$
   $\varphi_k : \ x_k - x_{k+1} = 0, \forall k \in \{1, \dots, d-1\}$
   $\varphi_d : \ x_{d-1} + x_d = 0.$

2. The vertices of $\sigma$ are:
   $u_0 = \left(0^{\{d\}}\right)$
   $u_1 = \left(1, 0^{\{d-1\}}\right)$
   $u_k = \left(\frac{1}{2}^{\{k\}}, 0^{\{d-k\}}\right), \forall k \in \{2, \dots, d-2\}$
   $u_{d-1} = \left(\frac{1}{2}^{\{d-1\}}, -\frac{1}{2}\right)$
   $u_d = \left(\frac{1}{2}^{\{d\}}\right).$

3. The minimal height falls on any of $\varphi_k$ for $k$ in $\{2, \dots, d-2\}$ and is equal to $h(\sigma) = \frac{1}{2\sqrt{2}}$ (see the augmented diagram in Figure 11).

4. The circumcentre of the simplex is $\left(\frac{1}{2}, 0, \frac{1}{4}^{\{d-4\}}, \frac{1}{2}, 0\right)$ and the circumradius is $R(\sigma) = \frac{\sqrt{d+4}}{4}$, which is easily verifiable. The incentre is $\left(\frac{1}{2}, \frac{d-2}{2(d-1)}, \frac{d-3}{2(d-1)}, \dots, \frac{1}{2(d-1)}, 0\right)$ and the inradius is $r(\sigma) = \frac{1}{2\sqrt{2}(d-1)}$, which is easily verifiable.

5. The longest edge is given by $\vec{u}_d - \vec{u}_0$ and is equal to $L(\sigma) = \frac{\sqrt{d}}{2}$.

6. The aspect ratio, the thickness and the radius ratio are:
$$\alpha(\sigma) = \frac{1}{\sqrt{2(d+4)}} \quad \text{and} \quad \theta(\sigma) = \frac{1}{\sqrt{2d}} \quad \text{and} \quad \rho(\sigma) = \frac{\sqrt{2}}{\sqrt{d+4}(d-1)}.$$

7. The volume of the simplex is:
$$vol(\sigma) = \frac{1}{d!} \det \begin{pmatrix} 1 & 1/2 & \dots & 1/2 & 1/2 & 1/2 \\ 0 & 1/2 & & 1/2 & 1/2 & 1/2 \\ 0 & 0 & \ddots & \vdots & \vdots & \vdots \\ \vdots & \vdots & \ddots & 1/2 & 1/2 & 1/2 \\ 0 & 0 & \dots & 0 & 1/2 & 1/2 \\ 0 & 0 & \dots & 0 & -1/2 & 1/2 \end{pmatrix} =$$
$$\frac{1}{2d!} \det \begin{pmatrix} 1 & 1/2 & \dots & 1/2 & 1/2 \\ 0 & 1/2 & \dots & 1/2 & 1/2 \\ \vdots & \ddots & \ddots & \vdots & \vdots \\ 0 & \dots & 0 & 1/2 & 1/2 \\ 0 & \dots & 0 & 0 & 1/2 \end{pmatrix} + \frac{1}{2d!} \det \begin{pmatrix} 1 & 1/2 & \dots & 1/2 & 1/2 \\ 0 & 1/2 & \dots & 1/2 & 1/2 \\ \vdots & \ddots & \ddots & \vdots & \vdots \\ 0 & \dots & 0 & 1/2 & 1/2 \\ 0 & \dots & 0 & 0 & 1/2 \end{pmatrix} = \frac{1}{2^{d-2}d!}.$$
   The fatness of the simplex is:
$$\Theta(\sigma) = \frac{vol(\sigma)}{L(\sigma)^d} = \frac{4}{d^{d/2}d!}.$$

8. Observe that the inner products of the normal vector $s_{d-2}$ to the hyperplane $\varphi_{d-2}$ with the circumcentre and $u_{d-2}$ have different signs:
$$\langle s_{d-2}, c \rangle = -\frac{1}{4} \quad \text{and} \quad \langle s_{d-2}, u_{d-2} \rangle = \frac{1}{2}.$$
   Therefore the hyperplane $\varphi_{d-2}$ separates the circumcentre from $u_{d-2}$, so by Theorem 4.5 the triangulation is not Delaunay.

9.

**Proposition B.6.**

*(a) The vertex set of a $\tilde{D}_4$ triangulation is a lattice.*

*(b) No other vertex set of a $\tilde{D}_d$ triangulation for $d \geq 5$ is a lattice.*

*Proof.* (a) A point $v \in \mathbb{R}^d$ is a vertex of the triangulation if and only if it lies in the intersection of at least $d$ hyperplanes in $\mathcal{H}$ (as defined in Section A.5) that are linearly independent. Equivalently, the inner products of at least $d$ linearly independent positive roots should be integers.

Let $E = \{e_1, ..., e_d\}$ be the canonical base of $\mathbb{R}^d$. Bourbaki [7, Planche IV] gives the explicit expressions of positive roots:

$$\begin{aligned} R^+ &= \{e_i - e_j \mid i,j \in \{1,\dots,d\} \text{ and } i<j\} \cup \\ &\quad \{e_i + e_j \mid i,j \in \{1,\dots,d\} \text{ and } i<j\}. \end{aligned}$$

Denote by $V$ the vertex set of the triangulation. Let $\Lambda = \{x \in (\frac{1}{2}\mathbb{Z})^4 \mid x_1 + x_2 + x_3 + x_4 \in \mathbb{Z}\}$. We will now prove that $V = \Lambda$.

For any $x \in \Lambda$, its image by an affine reflection $\sigma_{r,k}$ for $r \in R$ and $k \in \mathbb{Z}$, as defined in Section A.5, is $\sigma_{r,k}(x) = x - (\langle x, r\rangle - k)r^\vee$. For any $r \in R$ and $x \in (\frac{1}{2}\mathbb{Z})^4$, the inner product $\langle x, r\rangle$ is in $\frac{1}{2}\mathbb{Z}$, hence $(\langle x, r\rangle - k)$ is in $\frac{1}{2}\mathbb{Z}$ as well. The coefficients of the dual root $r^\vee$ are integers, so $(\langle x, r\rangle - k)r^\vee \in (\frac{1}{2}\mathbb{Z})^4$, hence $\sigma_{r,k}(x) \in (\frac{1}{2}\mathbb{Z})^4$. By assumption, the sum of coefficients of $x$ is an integer. For any $r \in R^+$ defined above, the sum of coefficients of $\frac{1}{2}r$ is an integer as well. Therefore $\sigma_{r,k}(x) \in \Lambda$. Now recall that one can obtain any simplex from another one by a series of affine reflections. All vertices of $\sigma$ are in $\Lambda$, so with the above observation we conclude that any vertex in $V$ is in $\Lambda$ as well.

To prove the other direction, observe that $\{e_1 + e_2, e_1 - e_2, e_3 + e_4, e_3 - e_4\}$ is a set of 4 linearly independent positive roots that have integer inner products with any element in $\Lambda$.

With both inclusions proven, we conclude that $V = \Lambda$, which is a lattice.

(b) Let $V$ be the the vertex set of the triangulation. We will now prove that $v = u_3 - u_2 = \frac{1}{2}e_3$ is not in the vertex set, which implies that $V$ does not form a lattice.

One can easily check that the positive roots that have integer inner product with $v$ are exactly:

$$\begin{aligned} &\{e_i - e_j \mid i,j \in \{1,\dots,d\} \setminus \{3\} \text{ and } i<j\} \cup \\ &\{e_i + e_j \mid i,j \in \{1,\dots,d\} \setminus \{3\} \text{ and } i<j\} \end{aligned}$$

and these roots span the vector space $\mathrm{Vect}(E \setminus \{e_3\})$, which is $(d-1)$-dimensional. Thus, there does not exist $(r_1, ..., r_d) \subseteq R^+$ that are linearly independent and have integer inner products with $v$. We therefore conclude that $v$ does not belong to $V$.

□

**$\tilde{\mathbf{E}}_6$**


Figure 12: The augmented Coxeter diagram for the $\tilde{E}_6$ triangulation and the notation of the facets of a corresponding simplex.

1. The delimiting hyperplanes of the fundamental simplex $\sigma$ can be defined as follows:

$$\begin{aligned} \varphi_0 &: \ \tfrac{1}{2}((x_1 + x_2 + x_3 + x_4 + x_5 + x_8) - (x_6 + x_7)) = 1 \\ \varphi_1 &: \ (x_1 + x_8) - (x_2 + x_3 + x_4 + x_5 + x_6 + x_7) = 0 \\ \varphi_2 &: \ x_1 + x_2 = 0 \\ \varphi_3 &: \ x_1 - x_2 = 0 \\ \varphi_4 &: \ x_2 - x_3 = 0 \\ \varphi_5 &: \ x_3 - x_4 = 0 \\ \varphi_6 &: \ x_4 - x_5 = 0 \end{aligned}$$

2. The vertices of $\sigma$ are (in $\mathbb{R}^8$) [12, Chapter 21]:

$$\begin{aligned}
u_0 &= \left(0^{\{8\}}\right) \\
u_1 &= \left(0^{\{5\}}, -\tfrac{2}{3}^{\{2\}}, \tfrac{2}{3}\right) \\
u_2 &= \left(\tfrac{1}{4}^{\{5\}}, -\tfrac{1}{4}^{\{2\}}, \tfrac{1}{4}\right) \\
u_3 &= \left(-\tfrac{1}{4}, \tfrac{1}{4}^{\{4\}}, -\tfrac{5}{12}^{\{2\}}, \tfrac{5}{12}\right) \\
u_4 &= \left(0^{\{2\}}, \tfrac{1}{3}^{\{3\}}, -\tfrac{1}{3}^{\{2\}}, \tfrac{1}{3}\right) \\
u_5 &= \left(0^{\{3\}}, \tfrac{1}{2}^{\{2\}}, -\tfrac{1}{3}^{\{2\}}, \tfrac{1}{3}\right) \\
u_6 &= \left(0^{\{4\}}, 1, -\tfrac{1}{3}^{\{2\}}, \tfrac{1}{3}\right)
\end{aligned}$$

3. The smallest height falls on $\varphi_4$ and is equal to $h(\sigma) = \frac{\sqrt{2}}{6}$ (see the augmented diagram in Figure 12).

4. The circumcentre is $(0^{\{2\}}, -\frac{1}{6}^{\{2\}}, \frac{1}{3}, -\frac{1}{3}^{\{2\}}, \frac{1}{3})$ and the circumradius is $R(\sigma) = \frac{1}{\sqrt{2}}$, which is easily verifiable. The incentre is $(0, \frac{1}{12}, \frac{1}{6}, \frac{1}{4}, \frac{1}{3}, -\frac{1}{3}, -\frac{1}{3}, \frac{1}{3})$ and the inradius is $r(\sigma) = \frac{1}{12\sqrt{2}}$, which is easily verifiable.

5. The longest edge is $L(\sigma) = \frac{2}{\sqrt{3}}$.

6. The aspect ratio, the thickness and the radius ratio are:

$$\alpha(\sigma) = \frac{1}{6} \quad \text{and} \quad \theta(\sigma) = \frac{1}{2\sqrt{6}} \quad \text{and} \quad \rho(\sigma) = \frac{1}{12}$$

7. The volume of the simplex $\sigma$ is: $vol(\sigma) = \frac{\sqrt{3}}{51840}$.
   Therefore, the fatness is:
$$\Theta(\sigma) = \frac{vol(\sigma)}{L(\sigma)^6} = \frac{\sqrt{3}}{174960} \sim 9.900 \cdot 10^{-6}$$

8. Observe that the inner products of the normal vector $n = (0^{\{3\}}, 1, 0^{\{4\}})$ to the hyperplane $x_4 = 0$ with the circumcentre and the vertices have different signs: the inner product $\langle n, c\rangle = -\frac{1}{6}$ is strictly negative, whereas the inner products $\langle n, u_i\rangle$ are all non-negative. Therefore the hyperplane $x_4 = 0$ separates the circumcentre from the rest of the simplex, so by Theorem 4.5 the triangulation is not Delaunay.

9. 

**Proposition B.7.** *The vertex set of a $\tilde{E}_6$ triangulation does not form a lattice.*

*Proof.* A point $v \in \mathbb{R}^8$ is a vertex of the triangulation if and only if it lies in the intersection of at least 6 hyperplanes in $\mathcal{H}$ (as defined in Section A.5) that are linearly independent. Equivalently, the inner products of at least 6 linearly independent positive roots should be integers.

Let $E = \{e_1, ..., e_8\}$ be the canonical base of $\mathbb{R}^8$. Bourbaki [7, Planche V] gives the explicit expressions of positive roots:

$$\begin{aligned}
R^+ \quad = \quad & \{e_j - e_i \mid i, j \in \{1, \dots, 5\} \text{ and } i < j\} \cup \\
& \{e_i + e_j \mid i, j \in \{1, \dots, 5\} \text{ and } i < j\} \cup \\
& \left\{ \frac{1}{2}\left(e_8 - e_7 - e_6 + \sum_{i=1}^{5} (-1)^{\nu(i)} e_i\right) \;\middle|\; \sum_{i=1}^{5} \nu(i) \text{ is even} \right\}.
\end{aligned}$$

Let $V$ be the vertex set of the corresponding triangulation. We will now prove that $v = -2u_1 + 3u_2 + 3u_3 - 2u_4 = \frac{3}{2}e_2$ is not in the vertex set, which implies that $V$ does not form a lattice.

One can easily check that the positive roots that have integer inner product with $v$ are exactly:

$$\begin{aligned}
& \{e_j - e_i \mid i, j \in \{1, 3, 4, 5\} \text{ and } i < j\} \cup \\
& \{e_i + e_j \mid i, j \in \{1, 3, 4, 5\} \text{ and } i < j\}
\end{aligned}$$

and these roots span the vector space $\mathrm{Vect}(\{e_1, e_3, e_4, e_5\})$, which is 4-dimensional.

Thus, there do not exist $(r_1, ..., r_6)$ that are linearly independent and have integer inner products with $v$. We therefore conclude that $v$ does not belong to $V$.

□


Figure 13: The augmented Coxeter diagram for the $\tilde{E}_7$ triangulation and the notation of the facets of a corresponding simplex.

### $\tilde{\mathbf{E}}_7$

1. The delimiting hyperplanes of the fundamental simplex $\sigma$ can be defined as follows:

$$\begin{aligned}
\varphi_0 &: \quad x_7 - x_8 = 1 \\
\varphi_1 &: \quad (x_1 + x_8) - (x_2 + x_3 + x_4 + x_5 + x_6 + x_7) = 0 \\
\varphi_2 &: \quad x_1 + x_2 = 0 \\
\varphi_3 &: \quad x_1 - x_2 = 0 \\
\varphi_4 &: \quad x_2 - x_3 = 0 \\
\varphi_5 &: \quad x_3 - x_4 = 0 \\
\varphi_6 &: \quad x_4 - x_5 = 0 \\
\varphi_7 &: \quad x_5 - x_6 = 0
\end{aligned}$$

2. The vertices of $\sigma$ are (in $\mathbb{R}^8$) [12, Chapter 21]:

$$\begin{aligned}
u_0 &= \left(0^{\{8\}}\right) \\
u_1 &= \left(0^{\{6\}}, \tfrac{1}{2}, -\tfrac{1}{2}\right) \\
u_2 &= \left(-\tfrac{1}{4}^{\{6\}}, \tfrac{1}{2}, -\tfrac{1}{2}\right) \\
u_3 &= \left(\tfrac{1}{6}, -\tfrac{1}{6}^{\{5\}}, \tfrac{1}{2}, -\tfrac{1}{2}\right) \\
u_4 &= \left(0^{\{2\}}, -\tfrac{1}{4}^{\{4\}}, \tfrac{1}{2}, -\tfrac{1}{2}\right) \\
u_5 &= \left(0^{\{3\}}, -\tfrac{1}{3}^{\{3\}}, \tfrac{1}{2}, -\tfrac{1}{2}\right) \\
u_6 &= \left(0^{\{4\}}, -\tfrac{1}{2}^{\{2\}}, \tfrac{1}{2}, -\tfrac{1}{2}\right) \\
u_7 &= \left(0^{\{5\}}, -1, \tfrac{1}{2}, -\tfrac{1}{2}\right)
\end{aligned}$$

3. The smallest height falls on $\varphi_4$ and is equal to $h(\sigma) = \frac{\sqrt{2}}{8}$ (see the augmented diagram in Figure 13).

4. The circumcentre is $(-\frac{1}{8}^{\{2\}}, 0^{\{3\}}, -\frac{1}{2}, \frac{1}{4}, -\frac{1}{4})$ and the circumradius is $R(\sigma) = \frac{1}{4}\sqrt{\frac{13}{2}}$, which is easily verifiable. The incentre is $(0, -\frac{1}{18}, -\frac{1}{9}, -\frac{1}{6}, -\frac{2}{9}, -\frac{5}{18}, \frac{17}{36}, -\frac{17}{36})$ and the inradius is $r(\sigma) = \frac{1}{18\sqrt{2}}$, which is easily verifiable.

5. The longest edge is $L(\sigma) = \sqrt{\frac{3}{2}}$.

6. The aspect ratio, the thickness and the radius ratio are:

$$\alpha(\sigma) = \frac{1}{2\sqrt{13}} \quad \text{and} \quad \theta(\sigma) = \frac{1}{4\sqrt{3}} \quad \text{and} \quad \rho(\sigma) = \frac{2}{9\sqrt{13}}$$

7. The volume of $\sigma$ is: $vol(\sigma) = \frac{\sqrt{2}}{2903040}$.
   Therefore, the fatness is:
$$\Theta(\sigma) = \frac{vol(\sigma)}{L(\sigma)^7} = \frac{\sqrt{3}}{14696640} \sim 1.179 \cdot 10^{-7}$$

8. Observe that the inner products of the normal vector $s_4$ to the hyperplane $\varphi_4$ with the circumcentre and the vertices have different signs: the inner product $\langle s_4, c\rangle = -\frac{1}{8}$ is strictly negative, whereas the inner products $\langle n, u_i\rangle$ are all non-negative. Therefore the hyperplane $\varphi_4$ separates the circumcentre from the rest of the simplex, so by Theorem 4.5 the triangulation is not Delaunay.

9. 

**Proposition B.8.** *The vertex set of a $\tilde{E}_7$ triangulation does not form a lattice.*

*Proof.* A point $v \in \mathbb{R}^8$ is a vertex of the triangulation if and only if it lies in the intersection of at least 7 hyperplanes in $\mathcal{H}$ (as defined in Section A.5) that are linearly independent. Equivalently, the inner products of at least 7 linearly independent positive roots should be integers.

Let $E = \{e_1, ..., e_8\}$ be the canonical base of $\mathbb{R}^8$. Bourbaki [7, Planche VI] gives the explicit expressions of positive roots:

$$\begin{aligned} R^+ \quad = \quad & \{e_j - e_i \mid i,j \in \{1,\dots,6\} \text{ and } i<j\} \cup \\ & \{e_i + e_j \mid i,j \in \{1,\dots,6\} \text{ and } i<j\} \cup \\ & \left\{ \frac{1}{2}\left(e_8 - e_7 + \sum_{i=1}^{6}(-1)^{\nu(i)} e_i\right) \;\middle|\; \sum_{i=1}^{6}\nu(i) \text{ is odd} \right\}. \end{aligned}$$

Let $V$ be the vertex set of the corresponding triangulation. We will now prove that $v = -6u_1 + 2u_2 + 3u_3 - 4u_4 = e_2$ is not in the vertex set, which implies that $V$ does not form a lattice.

One can easily check that the positive roots that have integer inner product with $v$ are exactly:

$$\begin{aligned} & \{e_j - e_i \mid i,j \in \{1,\dots,6\} \text{ and } i<j\} \cup \\ & \{e_i + e_j \mid i,j \in \{1,\dots,6\} \text{ and } i<j\} \end{aligned}$$

and these roots span the vector space $\mathrm{Vect}(\{e_1, ..., e_6\})$, which is 6-dimensional. Thus, there does not exist $(r_1, ..., r_7) \subseteq R^+$ that are linearly independent and have integer inner products with $v$. We therefore conclude that $v$ does not belong to $V$. □

**$\tilde{\mathbf{E}}_8$**

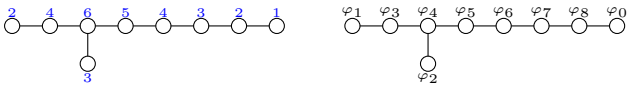


Figure 14: The augmented Coxeter diagram for the $\tilde{E}_8$ triangulation and the notation of the facets of a corresponding simplex.

1. The delimiting hyperplanes of the fundamental simplex $\sigma$ can be defined as follows:

$$\begin{aligned} \varphi_0 :&\quad x_7 + x_8 = 1 \\ \varphi_1 :&\quad (x_1 + x_8) - (x_2 + x_3 + x_4 + x_5 + x_6 + x_7) = 0 \\ \varphi_2 :&\quad x_1 + x_2 = 0 \\ \varphi_3 :&\quad x_1 - x_2 = 0 \\ \varphi_4 :&\quad x_2 - x_3 = 0 \\ \varphi_5 :&\quad x_3 - x_4 = 0 \\ \varphi_6 :&\quad x_4 - x_5 = 0 \\ \varphi_7 :&\quad x_5 - x_6 = 0 \\ \varphi_8 :&\quad x_6 - x_7 = 0 \end{aligned}$$

2. The vertices of $\sigma$ are [12, Chapter 21]:

$$\begin{aligned} u_0 &= \left(0^{\{8\}}\right) \\ u_1 &= \left(0^{\{7\}}, 1\right) \\ u_2 &= \left(\tfrac{1}{6}^{\{7\}}, \tfrac{5}{6}\right) \\ u_3 &= \left(-\tfrac{1}{8}, \tfrac{1}{8}^{\{6\}}, \tfrac{7}{8}\right) \\ u_4 &= \left(0^{\{2\}}, \tfrac{1}{6}^{\{5\}}, \tfrac{5}{6}\right) \\ u_5 &= \left(0^{\{3\}}, \tfrac{1}{5}^{\{4\}}, \tfrac{4}{5}\right) \\ u_6 &= \left(0^{\{4\}}, \tfrac{1}{4}^{\{3\}}, \tfrac{3}{4}\right) \\ u_7 &= \left(0^{\{5\}}, \tfrac{1}{3}^{\{2\}}, \tfrac{2}{3}\right) \\ u_8 &= \left(0^{\{6\}}, \tfrac{1}{2}^{\{2\}}\right) \end{aligned}$$

3. The circumcentre is $(-\frac{1}{12}^2, 0^5, \frac{1}{2})$ and the circumradius is $R(\sigma) = \frac{\sqrt{38}}{12}$, which is easily verifiable. The incentre is $(0, \frac{1}{30}, \frac{1}{15}, \frac{1}{10}, \frac{2}{15}, \frac{1}{6}, \frac{1}{5}, \frac{23}{30})$ and the inradius is $r(\sigma) = \frac{1}{30\sqrt{2}}$, which is easily verifiable.

4. The smallest height falls on $\varphi_4$ and is equal to $h(\sigma) = \frac{\sqrt{2}}{12}$ (see the augmented diagram in Figure 14).

5. The longest edge is $L(\sigma) = 1$.

6. The aspect ratio, the thickness and the radius ratio are:

$$\alpha(\sigma) = \frac{1}{2\sqrt{19}} \quad \text{and} \quad \theta(\sigma) = \frac{1}{6\sqrt{2}} \quad \text{and} \quad \rho(\sigma) = \frac{1}{5\sqrt{19}}$$

7. The volume of $\sigma$ is: $vol(\sigma) = \frac{1}{696729600} \sim 1.435 \cdot 10^{-9}$.

   Therefore the fatness is:

$$\Theta(\sigma) = \frac{vol(\sigma)}{L(\sigma)^8} = \frac{1}{696729600} \sim 1.435 \cdot 10^{-9}$$

8. Observe that the inner products of the normal vector $n = (0, 1, 0^{\{6\}})$ to the hyperplane $x_2 = 0$ with the circumcentre and the vertices have different signs: the inner product $\langle n, c\rangle = -\frac{1}{12}$ is strictly negative, whereas the inner products $\langle n, u_i\rangle$ are all non-negative. Therefore the hyperplane $x_2 = 0$ separates the circumcentre from the rest of the simplex, so by Theorem 4.5 the triangulation is not Delaunay.

9. 

**Proposition B.9.** *The vertex set of a $\tilde{E}_8$ triangulation does not form a lattice.*

*Proof.* A point $v \in \mathbb{R}^8$ is a vertex of the triangulation if and only if it lies in the intersection of at least 8 hyperplanes in $\mathcal{H}$ (as defined in Section A.5) that are linearly independent. Equivalently, the inner products of at least 8 linearly independent positive roots should be integers.

Let $E = \{e_1, ..., e_8\}$ be the canonical base of $\mathbb{R}^8$. Bourbaki [7, Planche VII] gives the explicit expressions of positive roots:

$$\begin{aligned} R^+ \quad = \quad & \{e_j - e_i \mid i, j \in \{1, \dots, 7\} \text{ and } i < j\} \cup \\ & \{e_i + e_j \mid i, j \in \{1, \dots, 7\} \text{ and } i < j\} \cup \\ & \left\{ \frac{1}{2}\left(e_8 + \sum_{i=1}^{7} (-1)^{\nu(i)} e_i\right) \;\middle|\; \sum_{i=1}^{7} \nu(i) \text{ is even} \right\}. \end{aligned}$$

Let $V$ be the vertex set of the corresponding triangulation. We will now prove that $v = -u_1 + 3u_2 + 4u_3 - 6u_4 = e_2$ is not in the vertex set, which implies that $V$ does not form a lattice.

One can easily check that the positive roots that have integer inner product with $v$ are exactly:

$$\begin{aligned} & \{e_j - e_i \mid i, j \in \{1, \dots, 7\} \text{ and } i < j\} \cup \\ & \{e_i + e_j \mid i, j \in \{1, \dots, 7\} \text{ and } i < j\} \end{aligned}$$

and these roots span the vector space $\mathrm{Vect}(\{e_1, ..., e_7\})$, which is 7-dimensional. Thus, there does not exist $(r_1, ..., r_8) \subseteq R^+$ that are linearly independent and have integer inner products with $v$. We therefore conclude that $v$ does not belong to $V$.

□

**$\tilde{\mathbf{F}}_4$**


Figure 15: The augmented Coxeter diagram for the $\tilde{F}_4$ triangulation and the notation of the facets of a corresponding simplex.

1. The delimiting hyperplanes of the fundamental simplex $\sigma$ can be defined as follows:

$$\begin{aligned}\varphi_0 :&\quad x_1 + x_2 = 1\\ \varphi_1 :&\quad x_2 - x_3 = 0,\\ \varphi_2 :&\quad x_3 - x_4 = 0,\\ \varphi_3 :&\quad x_4 = 0\\ \varphi_4 :&\quad x_1 - x_2 - x_3 - x_4 = 0\end{aligned}$$

2. The vertices of $\sigma$ are:

$$\begin{aligned}u_0 &= (0,0,0,0)\\ u_1 &= \left(\tfrac{1}{2},\tfrac{1}{2},0,0\right)\\ u_2 &= \left(\tfrac{2}{3},\tfrac{1}{3},\tfrac{1}{3},0\right)\\ u_3 &= \left(\tfrac{3}{4},\tfrac{1}{4},\tfrac{1}{4},\tfrac{1}{4}\right)\\ u_4 &= (1,0,0,0)\end{aligned}$$

3. The inverse height proportions suggest that the smallest height corresponds to $\varphi_2$ and is equal to $h(\sigma) = \frac{\sqrt{2}}{6}$ (see the augmented diagram in Figure 15).

4. The circumcentre of the simplex is $(\frac{1}{2}, 0, 0, 0)$ and the circumradius is $R(\sigma) = \frac{1}{2}$, which is easily verifiable. The incentre is $\left(\frac{6+5\sqrt{2}}{6(2+\sqrt{2})}, \frac{4+\sqrt{2}}{6(2+\sqrt{2})}, \frac{1}{6}, \frac{\sqrt{2}}{6(2+\sqrt{2})}\right)$ and the inradius is $r(\sigma) = \frac{\sqrt{2}}{6(2+\sqrt{2})}$, which is easily verifiable.

5. The longest edge is given by $\vec{u}_4 - \vec{u}_0$ and is equal to $L(\sigma) = 1$.

6. The aspect ratio, the thickness and the radius ratio are:

$$\alpha(\sigma) = \frac{\sqrt{2}}{6} \quad \text{and} \quad \theta(\sigma) = \frac{\sqrt{2}}{6} \quad \text{and} \quad \rho(\sigma) = \frac{\sqrt{2}}{3(2+\sqrt{2})}$$

7. The volume of $\sigma$ is: $vol(\sigma) = \frac{1}{576} = 0.00174$.
   Therefore the fatness is:
$$\Theta(\sigma) = \frac{vol(\sigma)}{L(\sigma)^4} = \frac{1}{576} \sim 0.00174$$

8. Observe that all inner products of the normals $s_i$ to hyperplanes $\varphi_i$ and the corresponding opposite vertices $u_i$ are positive. Observe as well that the inner products with the circumcentre $\langle s_i, c\rangle$ are either positive or zero. It implies that the circumcentre lies on the boundary of the simplex, therefore by Theorem 4.8 the triangulation is non-protected Delaunay.

9. **Proposition B.10.** *The vertex set of a $\tilde{F}_4$ triangulation does not form a lattice.*

   *Proof.* A point $v \in \mathbb{R}^4$ is a vertex of the triangulation if and only if it lies in the intersection of at least 4 hyperplanes in $\mathcal{H}$ (as defined in Section A.5) that are linearly independent. Equivalently, the inner products of at least 4 linearly independent positive roots should be integers.

   Let $E = \{e_1, ..., e_4\}$ be the canonical base of $\mathbb{R}^4$. Bourbaki [7, Planche VIII] gives the explicit expressions of positive roots:

$$R^+ = E \cup \{e_i \pm e_j \mid i, j \in \{1, \ldots, 4\} \text{ and } i < j\} \cup \left\{\frac{1}{2}(e_1 \pm e_2 \pm e_3 \pm e_4)\right\}.$$

   Let $V$ be the vertex set of the corresponding triangulation. We will now prove that $v = u_1 + u_2 = \left(\frac{7}{6}, \frac{5}{6}, \frac{1}{3}, 0\right)$ is not in the vertex set, which implies that $V$ does not form a lattice.

   One can easily check that the positive roots that have integer inner product with $v$ are exactly

$$\left\{e_4, e_1 + e_2, \frac{1}{2}(e_1 - e_2 - e_3 \pm e_4)\right\}.$$

   Note that $\frac{1}{2}(e_1 - e_2 - e_3 + e_4) = \frac{1}{2}(e_1 - e_2 - e_3 - e_4) + e_4$, so these roots are not linearly independent. Thus, there does not exist $(r_1, ..., r_4) \subseteq R^+$ that are linearly independent and have integer inner products with $v$. We therefore conclude that $v$ does not belong to $V$.

   □

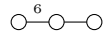


**$\tilde{G}_2$**

Simplex of $\tilde{G}_2$ triangulation (also called *Kisrhombille tiling*) is the right triangle with $\pi/6$ angle. By an easy computation, the aspect ratio, thickness and radius ratio are as follows:

$$\alpha(\sigma) = \theta(\sigma) = \frac{\sqrt{3}}{4} \quad \text{and} \quad \rho(\sigma) = \frac{1}{1+\sqrt{3}}$$

The fatness is $\Theta(\sigma) = \frac{\sqrt{3}}{8}$.

The circumcentre of any triangle lies on its hypotenuse, therefore by Theorem 4.8 the triangulation is non-protected Delaunay.

It is obvious from Figure 7 that the vertex set of the triangulation does not form a lattice.

# C Proofs of the optimal quality of regular simplices in each dimension

In this section we will prove Theorem 3.2. The proof will be subdivided into lemmas that prove that each individual quality measure we consider is maximized by the regular simplex.

**Radius ratio** The first result is by Klamkin for radius ratio [22]:

**Lemma C.1** ([22])**.** *Out of all $d$-simplices, the regular $d$-simplex $\Delta$ has the maximum radius ratio equal to $\rho(\Delta) = \frac{1}{d}$.*

**Aspect ratio** We can adapt the proof by Klamkin to prove the result for aspect ratio:

**Lemma C.2.** *Out of all $d$-simplices, the regular $d$-simplex $\Delta$ has the maximum aspect ratio equal to $\alpha(\Delta) = \frac{d+1}{2d}$.*

*Proof.* Let $\sigma$ be a $d$-simplex. We will now prove that $\alpha(\sigma) = \frac{h(\sigma)}{2R(\sigma)} \leq \frac{d+1}{2d}$ (see the augmented diagram).

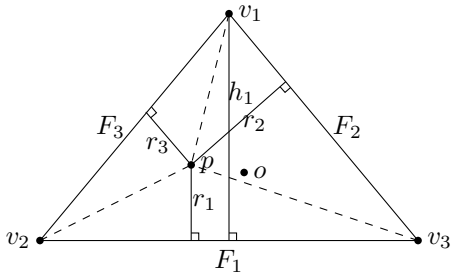


Figure 16: Illustration for the proof of Lemma C.2.

Let $F_i$ be the $(d-1)$-dimensional volume of the $i$th facet (see Figure 16). Denote $v_i$ the opposite vertex.

If $p$ is an arbitrary point, we have by Cauchy-Schwarz inequality:

$$\sum_{i=0}^{d} F_i \cdot \sum_{i=0}^{d} F_i \overrightarrow{pv_i}^2 \geq \left( \sum_{i=0}^{d} F_i \overrightarrow{pv_i} \right)^2 . \tag{2}$$

Note that the equality takes place if and only if $p$ is the circumcentre (making $\overrightarrow{pv_i}^2$ all equal).

Let $F = \sum_{i=0}^{d} F_i$, $o$ be the circumcentre and $\overrightarrow{oq} = \sum_{i=0}^{d} F_i \overrightarrow{ov_i}/F$. Then:

$$\sum_{i=0}^{d} F_i \overrightarrow{pv_i}^2 \quad = \quad \sum_{i=0}^{d} F_i \left(\overrightarrow{op} - \overrightarrow{ov_i}\right)\left(\overrightarrow{op} - \overrightarrow{ov_i}\right) = F\left(R(\sigma)^2 + \overrightarrow{op}^2 - 2\overrightarrow{op}\cdot\overrightarrow{oq}\right).$$

Since $2\overrightarrow{op}\cdot\overrightarrow{oq} = \overrightarrow{op}^2 + \overrightarrow{oq}^2 - \left(\overrightarrow{oq} - \overrightarrow{op}\right)^2 = \overrightarrow{op}^2 + \overrightarrow{oq}^2 - \overrightarrow{pq}^2$,

$$\sum_{i=0}^{d} F_i \cdot \sum_{i=0}^{d} F_i \overrightarrow{pv_i} = F^2\left(R(\sigma)^2 + \overrightarrow{pq}^2 - \overrightarrow{oq}^2\right). \tag{3}$$

Denote by $h_i$ and $r_i$ the distances from $v_i$ and $p$ respectively to the facet $F_i$.

Then $d(p, v_i)$ is greater than $h_i - r_i$ as the hypotenuse is greater than a leg in a right triangle (see Figure 16). So

$$\sum_{i=0}^{d} F_i \; d(p, v_i) \geq \sum_{i=0}^{d} F_i h_i - \sum_{i=0}^{d} F_i r_i.$$

Note that if $V$ denotes the volume of the simplex, then for a fixed $i$ we have $F_i h_i = dV$.

On the other hand, for all $i$, the $d$-simplex formed by $p$ and $F_i$ has a height $r_i$ with respect to $F_i$ (see Figure 16). It yields that $\sum_{i=0}^{d} F_i r_i = dV$. Therefore, $\sum_{i=0}^{d} F_i \; d(p, v_i) \geq (d+1)dV - dV = d^2 V$.

As before, let $h(\sigma) = \min_i h_i$. Now observe that

$$(d+1)dV = \sum_{i=0}^{d} F_i h_i \geq \sum_{i=0}^{d} F_i h(\sigma) = F h(\sigma),$$

hence

$$\sum_{i=0}^{d} F_i \; d(p, v_i) \geq \frac{dF h(\sigma)}{d+1}. \tag{4}$$

Thus combining (2), (3) and (4), we get:

$$F^2 \left( R(\sigma)^2 + \overrightarrow{pq}^2 - \overrightarrow{oq}^2 \right) = \sum_{i=0}^{d} F_i \sum_{i=0}^{d} F_i \overrightarrow{pv_i} \geq \left( \sum_{i=0}^{d} F_i \overrightarrow{pv_i} \right)^2 \geq \left( \frac{dF h(\sigma)}{d+1} \right)^2.$$

Setting $p$ equal to $q$ removes the $\overrightarrow{pq}$ term:

$$R(\sigma)^2 \geq \left( \frac{d}{d+1} h(\sigma) \right)^2 + \overrightarrow{oq}^2 \geq \left( \frac{d}{d+1} h(\sigma) \right)^2,$$

which gives the inequality that we sought to prove.

□

**Thickness** We can combine Lemma C.2 with Jung's theorem[21] to prove the result for thickness:

**Theorem C.3** (Jung's theorem)**.** *Let $S \subseteq \mathbb{R}^d$ be a compact set. Let $L(S)$ be its diameter and $R_{enc}(S)$ be the radius of the minimum enclosing ball. Then:*

$$R_{enc}(S) \leq L(S) \sqrt{\frac{d}{2(d+1)}}.$$

**Lemma C.4.** *Out of all $d$-simplices, the regular $d$-simplex $\Delta$ has the maximum thickness equal to $\theta(\Delta) = \sqrt{\frac{d+1}{2d}}$.*

*Proof.* Assume that $\sigma$ be a $d$-simplex. We will distinguish two cases: namely $\sigma$ is self-centred or not (as in Definition 4.1).

Let $\sigma$ be not self-centred. Let $\tau$ be a facet of $\sigma$ that separates $\sigma$ from its circumcentre $c$. Let $p$ be the vertex of $\sigma$ opposite to $\tau$. Denote by $h$ the height from $p$ to $\tau$ and $L$ be the length of the longest edge $e$ adjacent to $p$ (see Figure 17). By construction, $h \leq L/\sqrt{2}$, because the angle of the edge $e$ with $\tau$ is less or equal to $\pi/4$. Therefore:

$$\theta(\sigma) = \frac{h(\sigma)}{L(\sigma)} \leq \frac{h}{L} \leq \frac{1}{\sqrt{2}} \leq \sqrt{\frac{d+1}{2d}}.$$

From now on we assume that $\sigma$ is self-centred. This implies in particular that the circumradius of $\sigma$ is equal to the radius of the minimal enclosing ball of $\sigma$. So, by combining Lemma C.2 and Jung's theorem we get:

$$\theta(\sigma) = \frac{h(\sigma)}{L(\sigma)} = \frac{h(\sigma)}{2R(\sigma)} \frac{2R(\sigma)}{L(\sigma)} = \frac{h(\sigma)}{2R(\sigma)} \frac{2R_{enc}(\sigma)}{L(\sigma)} \leq \frac{d+1}{2d} \cdot 2 \sqrt{\frac{d}{2(d+1)}} = \sqrt{\frac{d+1}{2d}}.$$

Jung's theorem becomes equality in the case of the regular $d$-simplex [15], so its thickness is $\theta(\Delta) = \sqrt{\frac{d+1}{2d}}$. □

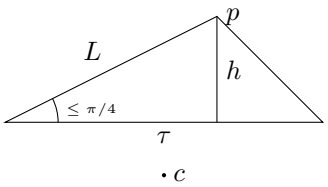


Figure 17: Illustration for the proof of Lemma C.4. The plane of the figure contains the edge of length $L$ and the height $h$. The intersection of this plane and the simplex is an obtuse triangle, and the angle adjacent to the longest edge is less than $\pi/4$.

**Fatness** Finally, we prove the result for fatness.

**Lemma C.5.** *Out of all $d$-simplices, the regular $d$-simplex $\Delta$ has the maximum fatness equal to $\Theta(\Delta) = \frac{1}{d!}\sqrt{\frac{d+1}{2^d}}$.*

*Proof.* Let $\sigma_d$ be a $d$-simplex. We define a sequence of faces $\sigma_1 \subset ... \subset \sigma_d$ of $\sigma_d$, such that for each $i \in \{1, ..., d-1\}$, $\sigma_i$ has dimension $i$ and the height falling on $\sigma_i$ is the minimum height in $\sigma_{i+1}$.

We can now express the volume of $\sigma$ in the following manner:

$$V(\sigma_d) = \frac{1}{d!}\prod_{i=1}^{d} h(\sigma_i).$$

Observe that for each $i$, the set of edges of $\sigma_d$ is a subset of the set of edges of $\sigma$, therefore we have $L(\sigma_i) \leq L(\sigma_d)$. By combining this fact with the volume expression we get:

$$\Theta(\sigma_d) = \frac{V(\sigma_d)}{L(\sigma_d)^d} = \frac{1}{d!}\prod_{i=1}^{d}\frac{h(\sigma_i)}{L(\sigma_d)} \leq \frac{1}{d!}\prod_{i=1}^{d}\frac{h(\sigma_i)}{L(\sigma_i)} = \frac{1}{d!}\prod_{i=1}^{d}\theta(\sigma_i).$$

From Lemma C.4, we have for each $i$, $\theta(\sigma_i) \leq \sqrt{\frac{i+1}{2i}}$. Therefore:

$$\Theta(\sigma_d) \leq \frac{1}{d!}\prod_{i=1}^{d}\sqrt{\frac{i+1}{2i}} = \frac{1}{d!}\sqrt{\frac{d+1}{2^d}}$$

and with that we conclude the proof. □

# D Proof of Lemma 4.4 and Lemma 4.7

*Proof of Lemma 4.4.* Let $\sigma$ be a simplex in $\mathcal{D}$ with circumsphere $S$, whose circumcentre is $c$ and circumradius $R$. We assume that the circumcentre $c$ lies outside of $\sigma$ and derive a contradiction. Because the circumcentre lies outside $\sigma$ there exists a facet $\tau$ of $\sigma$, whose supporting hyperplane $H_\tau$ separates $c$ from $\sigma$. We denote the simplex in $\mathcal{D}$ that shares the facet $\tau$ with $\sigma$ by $\sigma'$. We write $S'$ for the circumsphere of $\sigma'$ and denote its circumcentre by $c'$ and circumradius by $R'$. The $(d-2)$-dimensional sphere $T$ that forms the intersection of $S$ and $S'$, divides $S$ into a part that lies inside $S'$ and a cap that lies outside $S'$.

We shall call the line on which $c$ and $c'$ lie $\ell$. If we restrict to any two-dimensional plane $P$ that contains $\ell$, we see that $S \cap P$ and $S' \cap P$ are circles. We shall think of $\ell$ as vertical in $P$ (see Figure 18). The circumcentres can't coincide, because then they would lie on $H_\tau$. So the circles $S \cap P$ and $S' \cap P$ intersect transversely in two points. This means that $S \cap P$ is subdivided into two parts: a part inside $S' \cap P$ and a cap outside $S' \cap P$.

We shall assume that the cap lies below the part inside $S' \cap P$, see Figure 18. This implies that $c$ lies below $c'$ on $\ell$. This can be seen as follows: assume that both $S$ and $H_\tau$ are fixed. This means that points of intersection of $S \cap P$ and $S' \cap P$ are fixed, but the circumcentre $c'$ can be varied. We now let $c'$ descend along $\ell$ from $+\infty$ to $-\infty$. As long as $c$ and $c'$ do not coincide, the cap of $S \cap P$ outside $S' \cap P$ remains stable. At the point of coincidence of $c$ and $c'$ the inside and outside switch. It follows by considering the limit cases that the cap $S \cap P$ outside $S' \cap P$ lies below the cap inside as long as $c$ lies below $c'$ on $\ell$.

We now make two important observations. Firstly, because the triangulation $\mathcal{D}$ is Delaunay, the sphere $S'$ doesn't contain the vertex $p = \sigma \setminus \tau$. Hence $p$ lies on the cap of $S$ which is outside $S'$. Secondly, as we assume that the circumcentre $c$ lies outside of $\sigma$, $c$ lies above $H_\tau \cap P$.

Now let $o$ be the centre of $T = S \cap S'$ and let $q$ be a vertex of $\tau$. Because $d(c, o) < d(c', o)$, the distance $d(c, q)$ is strictly less than $d(c', q)$. By remarking that $d(c, q) = R$ and $d(c', q) = R'$, we get $R < R'$, which is a contradiction with the hypothesis that $R$ is the largest circumradius in $\mathcal{D}$.

□

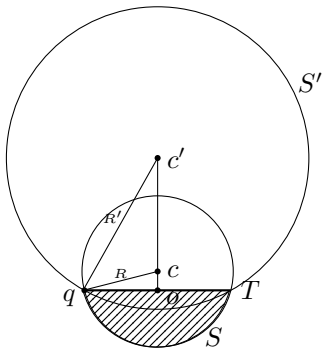


Figure 18: Construction for the proof of Lemma 4.4. The construction is confined to the plane containing the segments $[oc]$ and $[oq]$.

*Proof of Lemma 4.7.* We use the same construction and the same notations as in the proof of Lemma 4.4 (see Figure 18). Observe that by hypothesis $o$ coincides with $c$. If $c$ was different from $c'$, then the radius $R'$ would be bigger than $R$, which would lead to a contradiction. Therefore $c$ coincides with $c'$, so $\sigma$ and $\sigma'$ share the same circumball. We conclude the proof by observing that the vertex $\sigma' \setminus \tau$ lies on the circumball of $\sigma$, therefore $\sigma$ has zero protection. □

# E Comparison of quality measures between Coxeter triangulations

| $d =$ | 2 | 3 | 4 | 5 | 6 | 7 | 8 |
|---|---|---|---|---|---|---|---|
| $\tilde{A}_d$ | 1.000 | 0.949 | 0.894 | 0.845 | 0.802 | 0.764 | 0.730 |
| $\tilde{B}_d$ | - | 0.474 | 0.462 | 0.445 | 0.429 | 0.412 | 0.398 |
| $\tilde{C}_d$ | 0.666 | 0.612 | 0.566 | 0.527 | 0.495 | 0.468 | 0.444 |
| $\tilde{D}_d$ | - | - | 0.400 | 0.393 | 0.383 | 0.371 | 0.363 |
| $\tilde{E}_d$ | - | - | - | - | 0.286 | 0.243 | 0.204 |
| $\tilde{F}_d$ | - | - | 0.377 | - | - | - | - |
| $\tilde{G}_d$ | 0.577 | - | - | - | - | - | - |

Table 3: A comparative table showing the normalized aspect ratio $\hat{\alpha}$ value for Coxeter triangulations.

| $d=$ | 2 | 3 | 4 | 5 | 6 | 7 | 8 |
|---|---|---|---|---|---|---|---|
| $\tilde{A}_d$ | 1.000 | 0.949 | 0.894 | 0.845 | 0.802 | 0.764 | 0.730 |
| $\tilde{B}_d$ | - | 0.701 | 0.623 | 0.568 | 0.526 | 0.492 | 0.464 |
| $\tilde{C}_d$ | 0.828 | 0.717 | 0.641 | 0.584 | 0.540 | 0.505 | 0.475 |
| $\tilde{D}_d$ | - | - | 0.667 | 0.589 | 0.537 | 0.497 | 0.467 |
| $\tilde{E}_d$ | - | - | - | - | 0.500 | 0.431 | 0.367 |
| $\tilde{F}_d$ | - | - | 0.553 | - | - | - | - |
| $\tilde{G}_d$ | 0.732 | - | - | - | - | - | - |

Table 4: A comparative table showing the normalized radius ratio $\hat{\rho}$ value for Coxeter triangulations.

| $d=$ | 2 | 3 | 4 | 5 | 6 | 7 | 8 |
|---|---|---|---|---|---|---|---|
| $\tilde{A}_d$ | 1.000 | 0.891 | 0.864 | 0.807 | 0.781 | 0.743 | 0.721 |
| $\tilde{B}_d$ | - | 0.816 | 0.688 | 0.607 | 0.551 | 0.509 | 0.475 |
| $\tilde{C}_d$ | 0.760 | 0.648 | 0.579 | 0.529 | 0.491 | 0.461 | 0.436 |
| $\tilde{D}_d$ | - | - | 0.818 | 0.697 | 0.619 | 0.562 | 0.518 |
| $\tilde{E}_d$ | - | - | - | - | 0.528 | 0.422 | 0.363 |
| $\tilde{F}_d$ | - | - | 0.472 | - | - | - | - |
| $\tilde{G}_d$ | 0.707 | - | - | - | - | - | - |

Table 5: A comparative table showing the normalized fatness $\hat{\Theta}^{1/d}$ value for Coxeter triangulations.

| $d=$ | 2 | 3 | 4 | 5 | 6 | 7 | 8 |
|---|---|---|---|---|---|---|---|
| $\tilde{A}_d$ | 1.000 | 0.866 | 0.816 | 0.745 | 0.707 | 0.661 | 0.632 |
| $\tilde{B}_d$ | - | 0.500 | 0.447 | 0.408 | 0.378 | 0.354 | 0.333 |
| $\tilde{C}_d$ | 0.577 | 0.500 | 0.447 | 0.408 | 0.378 | 0.354 | 0.333 |
| $\tilde{D}_d$ | - | - | 0.447 | 0.408 | 0.378 | 0.354 | 0.333 |
| $\tilde{E}_d$ | - | - | - | - | 0.268 | 0.191 | 0.153 |
| $\tilde{F}_d$ | - | - | 0.298 | - | - | - | - |
| $\tilde{G}_d$ | 0.500 | - | - | - | - | - | - |

Table 6: A comparative table showing the normalized thickness $\hat{\theta}$ value for Coxeter triangulations.